Institut
de Ciències
Fotòniques

Neuron Guidance and Nano-Neurosurgery Using Optical Tools

Manoj V. Mathew

Barcelona, June, 2009

Universitat Politècnica de Catalunya

ICFO - Institut de Ciències Fotòniques

Chapter 3

Neuron Guidance

3.1 Overview

Neuron guidance is one of the most important aspect of neuroscience. During development of the nervous system, neurons project axons over long distances in order to reach their final targets. Along the way, growth cones located at the leading edges of axons detect and respond to environmental cues that guide them to their appropriate targets [86]. These guidance cues, both attractants and repellents, include contact-mediated or secreted molecules, acting over short or long distances, respectively. Axon guidance can be considered as the process of favored axon outgrowth towards or away from a particular region. Thus, axon guidance can be thought of as a process of biasing the extension/retraction of one side of the growth cone or axon shaft, compared to the other side [87]. This chapter discusses the structure of growth cones, the chemical basis of neuron guidance, various methods to externally induce neuron guidance and finally optical tools used in neuron guidance.

3.2 Structure of Growth Cones

Growth cone is the structure at the leading edge of the growing axon capable of sensing and rapidly responding to its environment [86]. The growth cone is responsible for generating forward tension on the elongating axon [88; 89]. Neuronal growth cones exhibit two primary domains characterized by two different types of cytoskeletal filaments: a central domain with microtubules that is generally continuous with the axon that precedes it, and a peripheral domain rich in actin filaments [89]. The peripheral domain is composed of actin-based structures called filopodia and lamellipodia that extend and retract many times faster than the rate of axon growth [90]. Figure 3.1 depicts the electron micro-graph of a developing neuron with growth cone.

Filopodia or microspikes are narrow cylindrical extensions capable of extending tens of microns from the periphery of the growth cone. Lamellipodia are flattened, veil-like extensions at the periphery of the growth cone [87]. The different regions of the growth cone include the peripheral (P) domain, composed primarily of lamellipodia and filopodia; the central (C) domain; composed of thicker regions invested by organelles and vesicles of varying sizes and the transitional (T) domain, a band of the growth cone at the interface

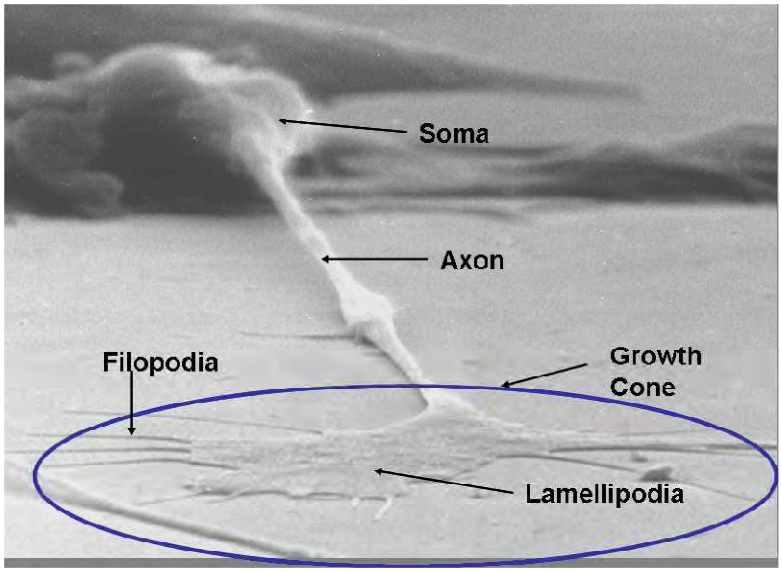

Figure 3.1: Electron-micrograph of a neuron with growth cone (www.biology.lsa.umich.edu/research/labs/ktosney)

of the P domain and C domains. [87]. Figure 3.2 shows a schematic representation of the various domains in the growth cone. The two principle cytoskeletal components in growth cones are actin filaments and microtubules. In developing peripheral nervous system neurofilaments are also present in the axon and C domain of the growth cone.

Actin filaments are helical polymers composed of actin monomers, often referred to as globular actin (G-actin). In growth cones, the barbed end of the actin filament generally faces the distal membrane and the pointed end faces the T region [87]. G-actin subunits assemble into long filamentous polymers called F-actin. Two parallel F-actin strands rotate 166 degrees in order and layer correctly on top of each other. This gives the appearance of a double helix and, more importantly, gives rise to microfilaments of the cytoskeleton. In growth cones, F-actin content is highest in the P and T regions of the growth cone and diminishes to varying levels in the C region of the growth cone [87]. The bulk of F-actin forms two types of arrays. A polarized bundled array of F-actin composes the core of filopodia and often extends proximally into the T region of the growth cone. F-actin can also adopt a meshwork-like array which forms the bulk of the lamellipodia in the P region of the growth cone [91]. Dynamic comet like structures that emanate from the T region and extend into the P region are termed intrapodia. Intrapodia are a hybrid of the bundled and meshwork arrays that compose the bulk of growth cone F-actin [92].

Microtubules are polarized structures composed of tubulin dimers assembled into linear arrays. Microtubules form a dense parallel array in the axon shaft. When they enter the growth cone, they generally splay apart. Microtubules can also adopt a looped morphology when growth cones are in a paused state [92]. To sprout new synaptic boutons, the microtubule loop would transiently break down, allowing microtubule polymerization and transport, followed by reformation of the loop at both the old and newly formed synaptic bouton.

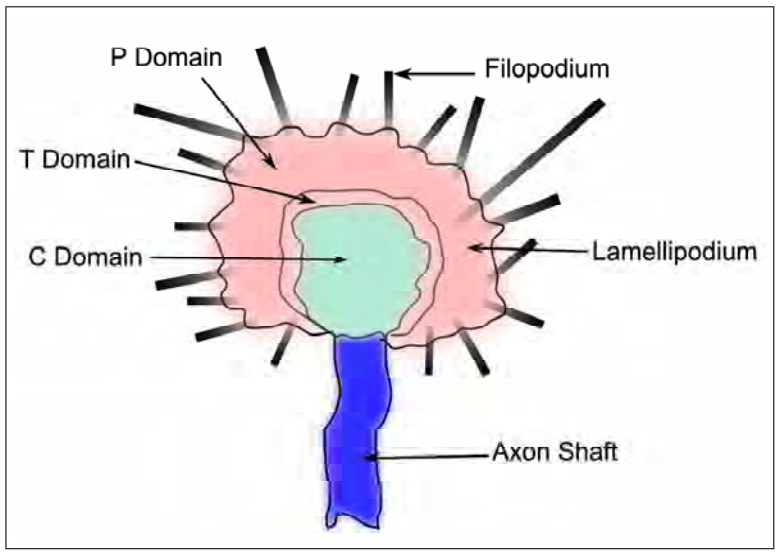

Figure 3.2: Schematic representation of the various domains in the growth cone

Actin filaments and MTs are in a constant state of flux. An essential feature of both polymers is that they are required by the cell to exist sometimes in a stable state and other times as dynamic structures. For neurons to extend long axons and dendrites and steer these processes to their eventual synaptic partners, they must exert precise control over the dynamics of both actin filaments and Microtubules. To accomplish these tasks, neurons contain a complex set of actin and MT-associated proteins in addition to the variety of isoforms and post-translational modifications.

3.3 The Clutch Hypothesis

The clutch hypothesis links together filopodial motility and actin dynamics [93]. Actin monomers in the peripheral domain of the growth cone, undergo constitutive plus end-directed filament assembly, elongating the filament in the distal tips of lamellipodia and filopodia and pushing the growth cone membrane in the forward direction; simultaneously the entire actin filament is dragged back by myosin-like molecular motors into the central domain where the actin filaments depolymerize [89; 94]. At the tail end of these actin filaments, the myosin-mediated retrograde flow blocks microtubules from advancing into the peripheral domain, and blocks the advance of the growth cone's central domain and therefore of the axon itself [95]. The balance of anterograde polymerization and retrograde retraction determines the advance of these actin-rich structures in the peripheral domain. When the rate of these two processes balance perfectly, the motor sits in neutral, and the growth cone neither advances nor retracts. This is the running motor of axon elongation, waiting to be engaged [89].

To engage the running motor the growth cone's grasp on an adhesive substrate must translate across the membrane and evoke the cytoskeletal changes needed for axonal growth. When the growth cone interacts with a substrate or cell-adhesion molecule, an increasingly strong connection is formed between the growth cones surface receptors and

the underlying actin network: the molecular clutch is engaged [89]. The link from membrane adhesion to actin cytoskeleton is sufficient to overcome the force created by myosin motors and retrograde flow is thereby decreased [96]. As actin polymerization continues at the leading edge, the balance is shifted toward forward protrusion of actin filaments in the tips of lamellipodia and filopodia. Simultaneously, the decrease in retrograde flow is accompanied by unimpeded microtubule polymerization into the peripheral domain, moving the central domain of the growth cone forward and thereby elongating the axon [89; 97]. Figure 3.3 shows the structure and dynamics of the growth cone.

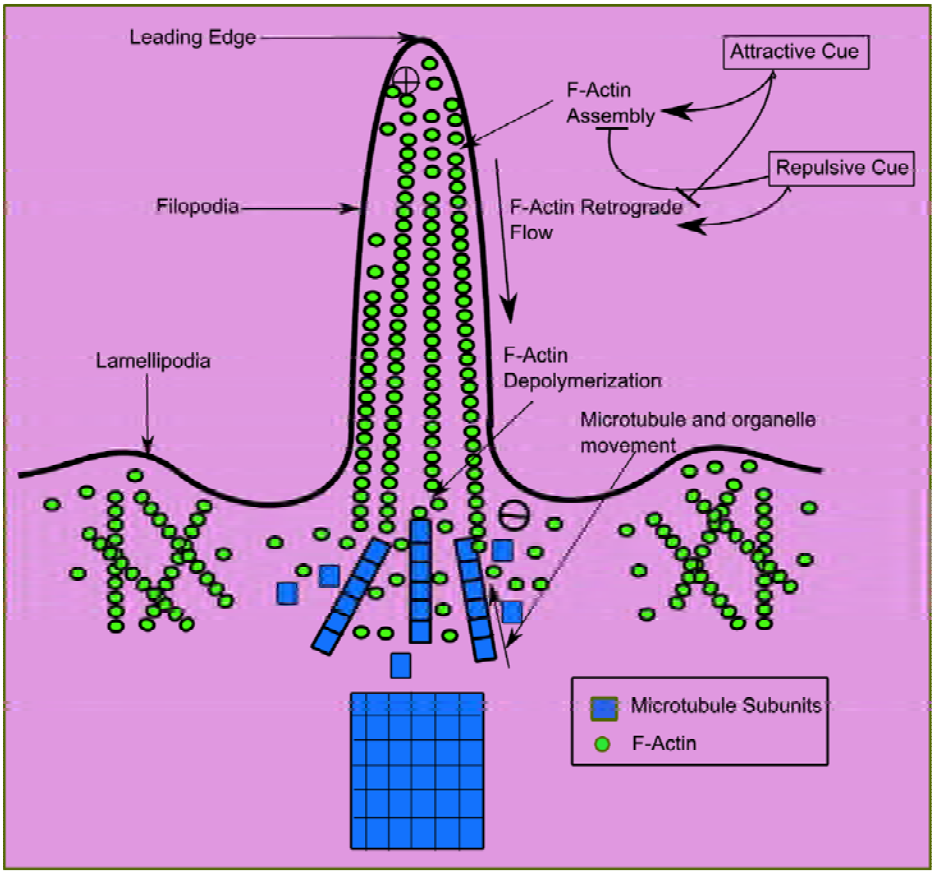

Figure 3.3: Schematic presentation of the growth cone dynamics

3.4 The Molecular Basis of Axon Guidance

Growing axons respond to guidance cues in the extracellular milieu. Axon growth, fasciculation, and steering are regulated by a wide range of attractive or repulsive axon guidance cues that can act over short or long distances. The growth cone detects and responds to axon guidance cues. The lamellipodia contain cross-linked F-actin filaments. The filopodia extend and retract through regulation of the rates of actin polymerization and depolymerization at the plus and minus ends of actin filaments, respectively, and of F-actin retrograde flow. Repulsive and attractive cues influence growth cone morphology

by regulating these processes [93]. The process of axon guidance involves the interplay between a large number of guidance cues (Biochemicals) of which the following are important: Rho GTPases, Netrins, Slits, Semaphorins, Ephrins, Receptor Protein Tyrosine Phosphatases, neurotrophins, Cell-Adhesion Receptors and Myelin-Associated Inhibitors: Nogo, MAG, OMgp. For a brief review of these guidance cues please refer to appendix A.1.

3.5 Neuron Degeneration and Regeneration

When the axon of a neuron is cut a series of degenerative changes are seen in the axon. The changes in the part of the axon distal to the injury are referred to as anterograde degeneration or Wallerian degeneration [98]. They take place in the entire length of that part of the axon. A few hours after injury axon becomes swollen and irregular in shape, and eventually breaks up into small segments. The region is invaded by numerous macrophages which remove degenerating axons, myelin and cellular debris. These macrophages probably secrete substances that cause proliferation of Schwann cells, which increase in size and produce a large series of membranes that help to form numerous tubes, which later play a crucial role in regeneration [98].

Degenerative changes in the neuron proximal to the injury are referred to as retrograde degeneration. These changes take place in the cell body and in the axon proximal to injury. The cell body of the injured neuron undergoes a series of changes that constitute the phenomenon of chromatolysis [98]. The cell body enlarges tending to become spherical. The nucleus moves form the center to the periphery. The nissl substance becomes much less prominent and appears to dissolve away: hence the term chromatolysis. Ultrastructural and histochemical alteration occur in the cell body. In some cases chromatolysis ends in cell death followed by degeneration of all its processes. The reaction is more severe when the injury to the axon is near the cell body [98].

It is sometimes observed that changes resulting from axonal injury are not confined to the injured neurons but extend to other neurons with which the injured neuron synapses. This phenomenon is called transneuronal degeneration [98]. The degeneration can extend through several synapses.

Changes in the proximal part of the axon are confined to a short segment near the site of injury. If the injury is sharp and clean the effects extend only upto one or tow nodes of Ranvier proximal to injury. If the injury is severe a longer segment of the axon may be affected. The changes in the affected part are exactly the same as described for the distal part of the axon. They are soon followed by active growth at the tip of the surviving part of the axon. This causes the terminal part of the axon to swell up. It then gives off a number of fine branches. These branches grow into the connective tissue at the site of injury in an effort to reach the distal cut end of the nerve. The Schwann cells of the distal part of the nerve proliferate to form a series of tubes. When one of the regenerating axonal branches succeeds in reaching such a tube, it enters it and then grows rapidly within it. The tube serves as a guide to the growing fiber [98]. Axonal branches that fail to reach one of the tubes degenerate. It often happens that more than one axonal branch enters the same tube. In that case the largest branch survives and the others degenerate.

The axonal terminal growing through the Schwann cell tube ultimately reaches, and establishes contact with, an appropriate peripheral end organ. Failure to do so results

in degeneration of the newly formed axon. The new axon formed in this way is at first very thin and devoid of a myelin sheath [98]. However there is progressive increase in its thickness and a myelin sheath is formed around it. The chances of regeneration of a cut nerve are considerably increased if the two cut ends are near each other, and if scar tissue does not intervene between them. The tubes formed by Schwann cells being to disappear if they are not invaded by axons for a long time.

Axons in the CNS donot regenerate as in peripheral nerves. This is primarily due to the differences in the myelin sheaths between central and peripheral systems. The central nervous system myelin is produced by oligodendrocytes. CNS neurons do not intrinsically lack an intrinsic ability to regenerate as they can extend long fibers through myelin-free spinal cord, grafts of peripheral nerves, or purified Schwann cell implants [99; 100]. The neurite growth in CNS is inhibited by Myelin Associated Inhibitor (MAIs) proteins expressed on oligodendrocyte surfaces that interact with axonal receptors [101; 102]. In addition the dense astrocytic scars present a barrier to growing neurites [103]. Astrocyte processes are tightly interlinked by junctions and could thus form a mechanical obstacle. Additionally, specific molecules with inhibitory functions are also expressed in these regions. In particular, it has been shown that after injury, reactive astrocytes express some of the same boundary molecules that are believed to restrict axonal growth during development [102].

3.6 External Means for Neuron Guidance

3.6.1 Using Electric–Field

Endogenous Electric Fields (EFs) are widespread in developing and regenerating tissues. These EFs arise due to the transepithelial voltage difference in different locations. The size, location and developmental timing of EFs are appropriate to influence cell behavior during nervous system development. It has been established that the disruption of naturally occurring EFs perturbs neural development while neurogenesis during embryonic development [104].

Electric field has been successfully employed as a means for guiding neurites from neurons of Xenopus laevis in a predetermined direction [105]. DC electric fields 0.1 to 10V/cm was applied using a pair of salt bridges made with culture medium gelled by 2% agar. It was observed that neurites facing the cathode showed accelerated growth, while the growth of those facing the anode was reduced. Moreover the neurites growing relatively perpendicular to the field axis were prompted to curve toward the cathode. The reversal of the polarity of the electric field led to a rapid reversal in the neurite orientation. It was also noted that the number of neurite-bearing neurons per culture and the average neurite length were increased. These effects were absent in cultures treated with electric fields of similar strength but alternating polarity and hence the role of a gradient of extracellular diffusible substances or the flow of culture medium as a result of the field were ruled out.

Cathodal accumulation of growth-controlling surface glycoproteins by the field was attributed as the underlying mechanism of the field-induced orientation of neurite growth toward the cathode. The effect of pulsed DC fields were also tested [106] and it was found that the extent of neurite orientation depended upon the duration, amplitude, and frequency of the pulse but appeared to be similar to that produced by a uniform DC field

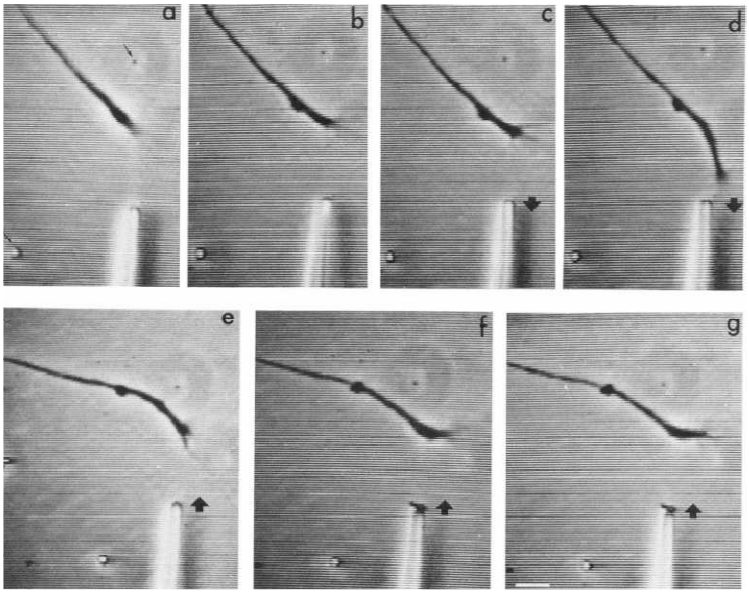

Figure 3.4: Bending of the growing tip of a neurite in response to a focally applied steady electric field. a-b control growth without electric field, c-d after application of a negative electric field, e-g after reversal of polarity [106].

of an equivalent time-averaged field intensity. Figure 3.4 shows the orientation of neurite growth in response to an applied electric field.

It has been demonstrated however that growth cones are attracted to or repelled by a cathode depending on the substratum [104; 107]. It also depends on whether the process is axonal or dendritic, and the nerve cell type [104; 108]. In addition to directing the growth cones, EFs can modify neuronal architecture by increasing and directing branching [109] and by selectively pruning some processes [110].

Pharmacological experiments have shown that cathodal attraction of Xenopus spinal growth cones involves the neurotrophin receptors trkB and trkC, the neuronal nicotinic ACh receptor (nAChR), receptor tyrosine kinases , phospholipase C, several isoforms of protein kinase C, extracellular Ca^{2+}, and Ca^{2+} from intracellular stores [104]. Moreover it has also been demonstrated that cAMP could act as a gating or regulatory molecule for the EF response, as it does for *in-vitro* chemotropic guidance, and that Ca^{2+} and cAMP might act as coordinate regulators of the directional field response [104; 111].

In addition it has been seen that EFs redistribute charged receptor proteins such as the epidermal growth factor (EGF) receptor [104; 112] and nAChR to the cathodal sides of cells. In general, these findings place an EF among the Group I chemotropic guidance cues (those that exert their effects through Ca^{2+} and cAMP; for example, netrin-1, NGF and myelin associated glycoprotein (MAG)) [104]. Interestingly, electrical activation of neural activity switches the repulsive chemotropic response to MAG to an attractive one [113]. A DC EF can also modulate other guidance cues. For example, a weak EF induces anodal attraction in the presence of neurotrophin-3 (NT3) but this switches to cathodal attraction if the EF is slightly stronger [104; 114].

3.6.2 Substrate Patterning

Nervous system development is strongly influenced by geometric patterns present within embryos during developmentally significant periods. Hence the the physical shape of the substratum induces alignment or directional growth of neuronal cells. This process is called contact guidance [115]. By building barriers or channels which would restrict the axonal growth trajectory, neurons can be let to grow (or not to grow) in a specific direction [116]. Neurons can be made to grow on scratched patterns etched onto quartz surfaces. This results in the growth cones orienting in the direction of the grooves [116; 117]. Dissociated embryonic Xenopus spinal cord neurons grow neurites parallel when grown on quartz etched with a series of parallel grooves [115]. Neurites grew faster in the favored direction of orientation and turned through large angles to align on grooves.

It has been observed that Dorsal Root Ganglion (DRG) neurons grow their neurites along magnetically aligned , 4mm diameter type-1 collagen rods [118]. When polymerized in a strong magnetic field, collagen fibers form in the direction of the magnetic field, producing long channels through which neurites can then be sent to grow [116]. The neurites were oriented more strongly in the direction of rods with increasing magnetic fields, apparently due to contact guidance response of growth cones at the neurite tips [118]. Similar works have also been performed on magnetically aligned fibrin gels, where chick DRG neurons were shown to align their neurites in the direction of the fibrin gels. The degree of alignment of neurites were found to be strongly dependent on the fibrin fibril diameter which in turn depended on the concentration of the Ca^{2+} in the fibrin forming solution [119].

Polyester microstructures can be used to form patterned neuronal networks [120]. Pits and grooves were fabricated on oxidized silicon chips using photolithography and baking. Cell bodies from pedal ganglia of the pond snail were placed into the pits and individual neurites grown along the grooves, and strong electrical synapses are formed between grown neurites. Patterned neuronal networks can also be formed by growing neurons on hydrogel-filled microscale tubes [121]. An acceleration of neurite outgrowth was observed in these conduits, which was found to be independent of the conduit diameter. A change in tissue architecture, with the cabling of cells within the microconduit was also observed.

The direction of neurite growth on patterned structures has been found to be dependent on the grove dimensions, neuronal type and cell age. While Hippocampal neurites grew parallel to deep grooves, they did so perpendicular to shallow, narrow ones [115]. Xenopus neurites sprouted from regions parallel to grooves but presumptive axons on rat hippocampal neurons emerged perpendicular to grooves and presumptive dendrites emerged parallel to them [115]. The frequency of perpendicular alignment of hippocampal neurites depended on the age of the embryos from which neurons were isolated, suggesting that contact guidance is regulated in development [115].

3.6.3 Substrate Patterning with Chemical Cues

Short-range chemical cues patterned onto substrates can be used to guide neurite extension. Short-range chemical cues are those which interact with a cell's membrane receptors directly and which do not have to travel as messengers from one point to another [116]. Neurons readily adhere to surfaces coated with extracellular matrix (ECM) proteins, as these best mimic the cells' natural environment in an organism. Peripheral

neurons from chick dorsal root and sympathetic ganglia and central neurons from retina and spinal cord when cultured on plastic substrata treated with purified laminin attached to and extended neurites [122]. However when the same experiment was performed with fibronectin only peripheral neurons initiated neurites. The guidance of neurites on 7-10 micron wide laminin pathways was found to be strongly correlated with the concentration of laminin initially applied to the substratum [123].

Rat hippocampal neurites have a high degree of attachment and control over guidance on substrates micropatterned with Poly-L-lysine (PLL) [124]. A modified microcontact printing technique was used to print μm-scale PLL patterns. Poly-L-lysine (PLL) is is a small polypeptide of the essential amino acid L-lysine, and is a cell adhesion molecule. PLL promotes neurite extension at a significantly slower rate than either laminin or fibronectin [116; 122]. When PLL and the cell adhesion molecule (CAM) L1 are patterned onto a substrate together, the somata preferentially adhere to the PLL, while neurites preferentially grow along the L1 [116; 125].

3.6.4 Localized Application of Guidance Cues

By applying localized sources of neuron guidance factors, growth cone turning behavior can be induced. A higher degree of localization is achieved by this process compared to diffusing these chemical cues in the media. This gives positional accuracy in the process of inducing guidance. A convenient way of doing this is by using microspheres coated with short range chemical cues and brought near the growth cones of neurons in culture. Beads can be held either mechanically or with a laser trap, and the forces exerted by the cell on the bead can thus be measured [116].

Polystyrene beads covalently conjugated to Nerve growth factor (NGF) can induce growth cone turning in chick DRG neurons [126]. Turning began with the formation of a stable contact of a filopodium or lamellipodium with an NGF-coated bead placed very near to the growth cone. This action was mediated by the high affinity of the NGF receptor trKA on the growth cone towards the NGF. In addition chemotropic guidance by NGF requires activation of the PLC and PI-3K pathways downstream of trk receptor activation [127].

The turning response of sensory neuron growth cones toward NGF-coated beads consists of three phases: (1) the initial filopodial contact is established, and within minutes the filopodium starts to thicken and darken, (2) cytoplasmic engorgement then occurs in the direction of the filopodial contact, and (3) the growth cone is consolidated, then reforms underneath the bead and continues extending in a new direction determined by the axis of interaction with the NGF-coated bead [126; 128]. It was also observed that F-actin ultimately protrudes past the coated bead, but the turning effect vanishes in the presence of vinblastine or taxol, two drugs which interfere with microtubule dynamics [116; 126–128].

Localized filopodia activity has been reported by contact of chick DRG neurons with NGF coated polystyrene beads [129]. Such localized activity is important in the formation of axon collateral branches. Beads coated with Immunoglobulin–G (IgG) and attached to the membranes of axons have been used to pull tethers from membranes of these axons by pulling the beads using optical tweezers [130]. The force applied on the tethers by the optical tweezers were used to measure the membrane tension.

Beads coated with anti-apCAM antibody have been used to investigate the mechanism

of translation of guidance cue recognition to cytoskeletal changes in Aplysia bag cell growth cones [96]. After placement, on the growth cone the beads rapidly bound to the cell surface and coupled to the underlying retrograde F-actin flow as they were restrained from further centripetal movement with a microneedle. After a latency period of about 10 min, an abrupt increase in the bead-restraining tension was observed accompanied by direct extension of the microtubule-rich central domain toward sites of apCAM bead binding. In addition the immunolocalization using an antibody against the cytoplasmic domain of apCAM revealed accumulation of the transmembrane isoform of apCAM around the bead-binding sites.

3.6.5 Mechanical Techniques

Mechanical forces may be used to pull the growth cone of axons in a particular direction. In an early work glass needles were attached to growth cones and pulled in 30-60-min steps of constant force (50-100μdyne) [131]. This resulted in an increased neurite elongation rate which was in turn proportional to the applied tension after a certain threshold. A high sensitivity of elongation rate increase of 1.5pm/hr per 1μdyne increase in tension was observed. It was also demonstrated that new neurite extensions can be initiated by the application of tension to the cell margin of chick sensory neurons. Initiation required tensions above some threshold and tension magnitudes. In related studies, when tension was applied to an axonal shaft perpendicular to the direction of extension, the neurite was observed to lengthen in response to the applied tension [116; 132].

A similar arrangement using glass needle to pulls growth cones was used to measure the cell adhesion forces associated with various cell adhesion molecules polylysine, laminin and or L1 [133]. Growth cones were detached from their culture surface by applying known forces with the calibrated glass needles and detachment force was taken as a measure of the force of adhesion of the growth cone to the substrate. It was observed that in all cases lamellipodial growth cones required significantly greater detachment force than filopodial growth cones. In addition it was observed that a significant difference in attachment forces for the different cell adhesion molecules were not observed with the exception of lamellipodial growth cones on Ll-treated surfaces, which had a significantly lower stress of detachment than on other surfaces.

Subjecting a growth cones membrane to tensile force has been shown to result in the activation of stretch-activated (SA) ion channels [116; 134]. In these studies, it was reported that when tension is applied to the cell membrane, the stretch-activated potassium ion channel has a higher probability of being open, which means that more potassium ions will be able to flow, which then results in the establishment of a voltage gradient across the cell membrane. This voltage gradient can then trigger voltage sensitive calcium channels to open, leading to an influx of calcium ions, which then leads to a turn away from the source of the stimulus if it is applied asymmetrically to the growth cone.

3.6.6 Optical Techniques

Using light to uncage calcium

Calcium ions are very important in the determination of cytoskeletal behavior, and regulation of Ca^{2+} ions in the growth cone is carried out by several classes of calcium channels. There are some which respond to voltage gradients, others to stretch activation, and yet others to the presence of other specific ion species [116]. If extracellular Ca^{2+} is

added to one side of a growth cone in normal culture medium, this induces an attractive turn, but when the cell medium lacks Ca^{2+} ions to begin with, this same introduction of Ca^{2+} to one side of a growth cone induces a repulsive turn [116; 135].

In an interesting work turning of nerve growth cones in Xenopus growth cones was induced by localized increases in intracellular calcium ions [135]. To spatially restrict cytosolic Ca^{2+} signals, focal laser-induced photolysis (FLIP) of o-nitrophenyl EGTA (NP-EGTA) was used to elevate $[Ca^{2+}]_i$ directly in a spot, 2μm in diameter. Fluo-3 was used as the calcium indicator to track dynamics of calcium activity. It was reported that a direct, spatially restricted elevation of intracellular $[Ca^{2+}]_i$ concentration on one side of the growth cone by focal laser-induced photolysis (FLIP) of caged Ca^{2+} consistently induced turning of the growth cone to the side with elevated $[Ca^{2+}]_i$ (attraction). Furthermore, when the resting $[Ca^{2+}]_i$ at the growth cone was decreased by the removal of extracellular Ca^{2+}, the same focal elevation of $[Ca^{2+}]_i$ by FLIP induced repulsion. These results provided direct evidence that a localized Ca^{2+} signal in the growth cone can provide the intracellular directional cue for extension and is sufficient to initiate both attraction and repulsion.

The spatial and temporal correlation between Ca^{2+} concentration and the regulation of filopodial growth has been investigated [136]. In this work the soma of B5 neurons from the pond snails, *Helisoma trivolvis* were injected simultaneously with o-Nitrophenyl EGTA and Calcium Green-1 to uncage calcium and simultaneously monitor the resulting changes in $[Ca^{2+}]_i$. An uncaging stimulus of 0.3-0.5s duration from the 351nm and 364nm lines of the UV laser localized to the center of a single growth cone elicited an immediate increase in $[Ca^{2+}]_i$ and a rapid return toward pretreatment levels within a couple of seconds. It was observed that regional uncaging of calcium in the lamellipodium caused a regional increase in $[Ca^{2+}]_i$, but induced filopodial elongation on the entire growth cone. Elevation of $[Ca^{2+}]_i$ locally within an individual filopodium resulted in the elongation of only the stimulated filopodium. These findings suggested that the effect of an elevation of $[Ca^{2+}]_i$ on filopodial behavior depends on the spatial distribution of the calcium signal. In particular, calcium signals within filopodia can cause filopodial length changes that are likely a first step towards directed filopodial steering events seen during path finding.

Direct use of light

Light has been used directly as a tool to guide axons in neurons [137]. This experiment used PC12 cells (a rat neuron precursor cell line, stimulated to spread with neuronal growth factor (NGF)) and NG108 cells (an immortalized mouse neuroblastoma rat glioma hybrid cell line). Control over the extending growth cone was achieved with a Ti:sapphire laser (800 nm). The laser light was guided and focused through the beam pathway of an inverted confocal microscope. The spot size diameter was varied in the plane of the lamellipodium between $\approx$2 and 16μm. The power directly measured after the microscope objective varied from 20 to 120mW. Variation in beam diameters $<$4μm was achieved by optically defocusing the beam and larger spot sizes were simulated by scanning the beam at a frequency of $\approx$0.1Hz along the desired area of the growth cones leading edge. Scanning at a frequency faster than intracellular processes generated an illuminated band along the lamellipodial outline. To achieve optical guidance, the beam was interactively steered with the confocal scanning microscope or by moving the microscope stage relative to the sample with an xy-piezo stage.

Optical guidance of neurons was observed to be a robust effect, successful for both rat

and mouse neuronal cell lines and a broad range of laser powers. Successful biased growth was characterized by a lamellipodia extension in the radius of influence (approximately three laser beam radii) that grew toward the beam center. The laser beam was asymmetrically positioned to the left or right of the leading edge of a growth cone, and exhibited clear attraction effects on the axons. It was observed that extending lamellipodia grow into the focus of the laser beam in 79.5% of the experimented cases. Figure 3.5 shows two of the successful guidance experiments. It was also observed that the laser increased

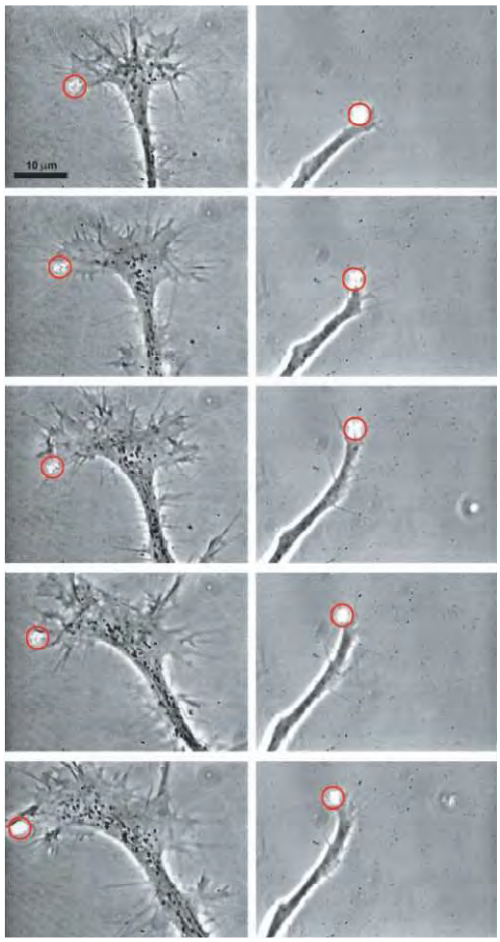

Figure 3.5: Time sequences of optically guided turns of neurons and optically enhanced neuronal growth. Optically induced turns are shown for a time period of 40 min (Left) and 20 min (Right) [137].

the rate at which the nerves leading edge advance. It was estimated that the lamellipodia extension rate increased from $7\pm3\mu$m/h to $37.5\pm22.5\mu$m/h. The biased growth events were transient, lasting a few minutes. However, their cumulative effect led to permanent results. Continuous optical guidance of the spreading growth cone resulted in controlled turns. Optically guided turns were achieved with a success rate of 85.0% whereas in control experiments with an imaginary laser spot the success rate for apparent optically guided turns was only 20%.

It was postulated that the power levels used were below those that could create gradient forces of the optical trap in the conventional fashion, whereby the tweezing effect of the trap is used to move an entire structure. Also the power levels were deemed to be low enough to avoid any significant heating that would bias the actin polymerization. It was indicated that the laser spot influences the general actin-based processes for growth cone extension during optically guided turns. The optical forces could interact with the proteins of the cytoplasm. Because the larger filamentous structures of the cytoplasm are crosslinked and coupled to the plasma membrane by focal adhesions, the optical forces could only exert a tension on these structures, but could not move them. However, globular proteins and small oligomeric structures are free to move in the cytoplasm, and thus the optical forces can impact their diffusive behavior. The smallest forces are felt by globular proteins and were suggested to be a lower bound for this effect. More over it was suggested that the laser beam, placed just outside the growth cone, creates an intensity gradient for the globular proteins of the cytoplasm, such as actin monomers, and they feel a weak optical dipole force. This force is directed toward the center of the laser spot.

The mechanism hence of light induced growth cone turn was proposed as follows. The optical gradient enhances actin polymerization at the leading edge by pooling actin monomers and providing nucleation seeds in the form of actin filament fragments. The resulting locally enhanced actin polymerization promotes a turn of the lamellipodium in the direction of optically increased actin density. Optical forces on the membrane might also allow actin monomers to flow into new extensions. Furthermore, although they cannot move the crosslinked actin cortex, the optical forces do pull on this actin network and relieve pressure at the rearward cortex-microtubule junction, thus enhancing pressure-dependent microtubule polymerization.

In a related work a line optical tweezers based approach was adopted to achieve axon guidance using light [138]. Instead of using a defocused laser beam approach (as in [137]), this work exploited an asymmetric intensity distribution along the major axis of the elliptical trap beam to guide transport of actin monomers in the desired direction. The N1E-115 cell line (derived from a subclone of C-1300 spontaneous mouse neuroblastoma tumor) was utilized for these experiments. The output from a 1064 nm, TEM00 mode, linearly polarized cw Nd:YAG laser was coupled to a high NA microscope objective through a cylindrical lens to yield an elliptical focal spot. An asymmetry was created in the intensity distribution of the trap beam by tilting the laser beam with respect to the axis of the cylindrical lens. The depth and the asymmetry of the potential well could then be controlled by control of the trap beam power and by changing the angle of incidence of the laser beam with respect to the optical axis of the microscope objective.

To bias the growth of the neuron, the cell body of the neuron was brought near the high-intensity gradient end of the elliptical focus so that the tip of the growing edge was closer to the lower gradient force. The direction of transport was chosen arbitrarily for induction of new growth cones. It was observed that compared with a growth rate of 11μm/h observed for unexposed neurons, the lamellipodia extension rate in the neuron subjected to line tweezers was estimated to be 32$\pm$6m/h. Irradiation of the neuron with a point tweezers having the same power (120mW) did not show any enhancement of growth. In addition the asymmetric transverse gradient force was also used to induce protrusions from the neuronal cell body. For short exposures, the optically induced protrusions were found to be transient, lasting a few minutes. However, with prolonged ($\approx$20 min) application of

asymmetric transverse gradient force, permanent growth cones were shown to be induced.

In another work [139] a direct comparison was made between the two previous works reported in [137] and [138]; studies which were performed on two independent optical set-ups and on differing cell-types at different temperatures and at different wavelengths. The aim of the work was to compare the two previous works on the same optical set-up, the same cell-type and at two different wavelengths on a large number of cells. Experiments were performed using NG108 cell lines and efficiency of light to guide axons were tested for two wavelengths 780nm and 1024nm at power levels ranging between 8-22mW at the focus. The ability to change the growth cone direction, by at least 30 degrees away from the original direction of neuron growth travel was used as the metric to measure the efficiency. It was found that the infra-red region of light was not damaging to the cells, and was able to manipulate cellular growth. There also appeared to be no difference between 780 nm and 1064 nm wavelengths of light in inducing this phenomenon with similar beam shapes at both wavelengths. The cells that responded were those which were already actively growing.

In order to investigate if the light was creating substantial amount of heating that could bias the actin polymerization in the growth cone, a temperature measurement was carried out using a dual-beam optical tweezers system. 660nm was used for trapping (2μm silica beads in water), together with either a 780nm or 1064nm with 15mW at the focus. At a room temperature of 25^0 for the case of using only the 660nm trapping laser, a temperature of 26.4 ± 1.5^0C and 28.1 ± 2.3^0 in the presence of the 780 nm and 1064 nm lasers respectively was measured. Other than the apparent differences in heating capability these results showed that neither wavelength causes sufficient heating to affect the rate of actin polymerization within cells held at 37^0.

A follow up work [140] on one of the previous works [138] on optically guiding axons, using line optical tweezers, has also been done. Experiments were performed upon the NG108 cell lines using 1064nm wavelength. To produce the asymmetric line profile, the beam was focused through a cylindrical lens and then truncated by a beam block at the focus resulting in an asymmetric beam of dimensions 1μm x 45μm and of total power 35–70mW at the sample plane. This experiment was designed to explore in detail the optical bias generated by the asymmetric line trap. If such a trap could enhance growth by biasing the flow of actin, as was previously suggested [138], then one would expect to observe a retardation of growth if the bias of the trap is reversed to drive actin away from the leading edge. However, such a retardation was not observed and in experiments designed to retard growth, guidance was actually observed to increase with the same efficiency as a forward bias configuration of the beam. The growth cones were observed to change direction from their initial trajectory to line up with the major axis of the beam regardless of the orientation of the asymmetry. A symmetric beam (no bias in either direction) used as a control also showed the same efficiency as both asymmetric configurations.

This work [140] also reported that on a number of experimental occasions the filopodia from an extending growth cone were clearly seen to align themselves with the major axis of the line trap as they grew outwards. This was independent of the asymmetrical bias orientation. This was attributed to the optical forces attracting the filopodia. Since filopodia are fundamental in determining which direction a growth cone will grow it was proposed that such aligning of the filopodia was an important mechanism for optically guided neuron growth. This therefore supports previous suggestions that the filopodia are

influenced by laser light.

Some works have also mathematically modeled the dynamics of neuronal growth as well as optical torques acting on filopodia exposed to focused NIR light sources. In an earlier work the neuronal growth was described as a result of a bistable stochastic process [141] and a mathematical model developed for the same. This bistable stochastic process was described as what controls the polymerization at the leading edge of the lamellipodium. Theoretical models have also been predicted for the optical forces acting on the growth cone [137; 140].

The weak dipole force experienced by the globular actin monomers in the cytoplasm when the laser beam, placed just outside the growth cone, creating an intensity gradient for the globular proteins, can be described by the expression [137]:

$$F(r)_{dipole} =<\mid p \mid \nabla \mid E(r,t) \mid>_{timeaverage}= \frac{1}{4}\alpha\nabla \mid E(r) \mid^2= \frac{\alpha\nabla I(r)}{2n_{cyt}\epsilon_0 c} \tag{3.1}$$

Here F is the force, E the electric field, α is the polarizibility of the protein experiencing the dipole force, n_{cyt} is the refractive index of the cytoplasm, ϵ_0 is the is the dielectric constant, c is the speed of light and I(r) represents the Gaussian intensity profile of the laser beam. This force is directed toward the center of the laser spot [137]. A significant portion of the cytoplasmic proteins, including G-actin, undergo Brownian motion within the cell, and their diffusive transport to the leading edge of a lamellipodium is essential for cell motility. By approximating the dipole force F_{dipole} with a spatially constant force equaling the dipole force at half the radius of the laser spot, a drift velocity caused by the dipole force toward the center of the laser beam can be estimated. This drift velocity biases diffusion of cytoplasmic proteins toward the laser [137]. The drift velocity, ν_{Drift} is given by [137]:

$$\nu_{Drift} = F_{dipole}/\zeta \tag{3.2}$$

Where $\zeta = K_B/D$, where K_B is the Boltzmann's constant and D is the diffusion constant of the globular protein.

By assuming that a filopodium is made up of a bundle of approximately 20-30 actin filaments, 10nm apart and up to 2μm in length and that a filament consists of a helical structure of actin dimers with a 74 nm pitch containing 14 dimers, the optical torque on the filopodium has been calculated by summing all the individual torques calculated with respect to one end of the filopodium [140]. Here the filopodium was considered to have approximately 19,000 monomers. The torque acting on multiple filopodia were then modeled as being free to turn around one of their ends, i.e. like a rod with a pivot point representing the end of the filopodium linked to the cell body. The optical forces and torques were calculated for several positions and orientations of the filopodium with respect to the laser beam. It was observed that the torque varies with the angle of the filopodium. Attractive equilibrium angular positions are reached when the optical torque changes from positive to negative as the angle of the filopodium increases. In the case of a circular Gaussian beam, it was observed that there exists only one equilibrium angle, whereas for the line trap there are two [140].

Chapter 4

Biological Samples

4.1 Overview

This chapter discusses the biological samples used in experiments described in this thesis and their culture methods. For the first series of experiments neurons form cerebral cortex of mouse embryos were used. The initial part of this chapter hence describes basic cell culture methods and subsequently protocols involved in culturing neuronal cells form mouse embryos. The later experiments described in this thesis use the model organism *C.elegans*. The later part of this chapter hence describes the basic biology of *C.elegans* and also looks into the muscular and nervous systems of this model organism. The final part of the chapter describes the *C.elegans* culture methods.

4.2 Basic Cell Culture Methods

4.2.1 Equipments

Cell culture preparations require a sterile environment to prevent atmospheric agents like bacteria from contaminating them. A hood can be used for such purpose. Horizontal flow hoods blow filtered air through a contained space directly at the user [142]. The air flow pushes the atmospheric particles away from the working area providing a good degree of protection from contamination. These hoods however donot prevent the user form getting infected if working with contagious bio-material. Laminar flow hoods which blow a curtain of blowing air vertically in front of the user with a glass barrier between the user and hood work space need to be used in such cases [142]. When working with highly infectious agents, a glove box in the place of the opening of the hood provides higher degree of protection [142]. The air in such hoods are either reflown after passing it through a series of filters or exhausted outside the laboratory though building ducts. Most laminar flow hoods are available with ultraviolet (UV) light fixtures for sterilization of the work space when not in use [142].

Incubators are required for maintaining cell cultures over long periods under prescribed conditions of temperature, sterility, humidity and pH. A water jacketed CO_2 chamber with removable shelves inside, control for gas flow, a pan in the bottom for water, a water jacket heater and a thermostat with overheating protection is the simplest and reliable option

[142]. The shelves and inside of the incubator are periodically sterilized manually using alcohol. Some incubators come equipped with build in UV sterilization facility.

All the media, glassware and other equipments used for cell culture need to be properly sterilized before use. An autoclave that generates its own steam is essential for such purpose [142]. These devices can be programed to sterilize for a given amount of time using a set temperature. Different sterilization programs are used depending on the type of media/device that needs to be sterilized.

Water baths, centrifuges, vortexers, freezers and refrigerators are also essential parts of a cell culture laboratory. Water bath are used for heat shocks or thawing of frozen reagents or samples. They could be a major source of contamination and need to be periodically cleaned and an antimicrobial detergent added [142]. Centrifuges are used for centrifugation, usually for separation of components of a suspension. They are designed to spin stably at very high spin rates. Centrifuges can be programmed to control the spin rate, time and temperature. Vortex machines are used to mix samples usually in small tubes. These machines usually have programmable vibration rates. Media, reagents and other chemicals need to be stored usually at temperature lower than the room temperature. Depending on the type they may need either to be stored in a refrigerator with temperature usually set at 6-7^{0}C or in a freezer with temperature of -20^{0}C. Long term storage of cells and some reagents often need a cryo freezer with a temperature of -80^{0}C.

4.2.2 Materials

The media commonly used in cell culture include Ham's F12, Dulbecco-modified Eagle's medium (DMEM), RPMI 1640, MCDB media, and combinations of these media, as well as sterile solutions of trypsin-EDTA, PBS, HBSS, etc:. Purchased liquid media might have undergone a period of storage so making media fresh from a powdered formulation is preferable [142]. Most media can be stored in a refrigerator but should be frozen for long term use. Some media however can precipitate upon freezing because of relatively high calcium and phosphate concentrations. Serum like Normal Horse Serum (NHS), Fetal Bovine Serum (FBS), Fetal Calf Serum (FCS) etc: might be needed as a supplement in some media preparations. Serum can be stored long term at -70 to -90^{0}C [142]. Use of serum can in some cases be avoided by the use of purified growth factors or hormones.

Plastic disposable cell culture materials such as pipettes, pipette tips, stirrers, spreaders etc: are preferable. If reusable glassware is used they need to be properly sterilized before use in cell culture procedures.

4.2.3 Conditions for cell culture

One of the primary requirements in cell culture is the culture medium. Nutrients that are essential for dividing cells, such as amino acids, fatty acids, sugars, ions, trace elements, vitamins and cofactors, ions and molecules necessary to maintain the proper chemical environment for the cell is provided by the medium [142]. Buffering system required to maintain a physiological pH and osmolarity are also provided in the culture medium [142]. An energy source usually glucose is also provided in the medium. In addition to having a nutritional role, amino acids and glucose, as well as ions such as NaCl, contribute to the osmolarity of the medium [142]. Most media also contain phenol red as a pH indicator.

Dulbecco's Modified Eagle's Medium (DMEM) is principally used with serum supple-

mentation for high-density growth of cells [142]. In contrast, Hams nutrient mixtures F12 and F10 and the MCDB series of media were tailored specifically for growing a specific cell type (e.g., CHO, fibroblasts), at low density with a minimal amount of undefined protein added [142]. The F12/DME medium is principally used for growing cells in defined serum-free conditions [142]. Fl2/DME medium works well for growing cells at low or high densities and in defined hormone-supplemented conditions or with serum. Leibovitz L-15 medium is used when cells need to be maintained outside the CO_2 incubator for long periods of time.

pH is the next important factor in maintaining good cell cultures. Glucose metabolism by the cells drives the pH of the medium basic which is observed as a change in color (red to pink) of the pH indicator phenol red. This can hinder proper cell growth. Buffering agents like Sodium Bicarbonate maintain an equilibrated pH in presence of CO_2. Each medium is formulated with components designed to work with a specified CO_2 concentration (most ranging from 0 to 10% CO_2/air mixtures) to give a pH of 7.0-7.4 [142]. Other buffering agents like HEPES help in maintaining physiological pH despite changes in carbon dioxide concentration (produced by cellular respiration) when compared to bicarbonate buffers.

Temperature is a very important factor in obtaining good cell cultures. Most cells have a physiological temperature at which they grow best. This temperature is usually 37^0C for most cell cultures.

4.3 Cultures from mouse cerebral cortex

Low density primary neuronal cell cultures as used in the initial set of experiments descried in this thesis were obtained from the cerebral cortex of CD1 mouse embryos at 15 days gestation (E15). The following procedure was carried out to obtain the cultures.

4.3.1 Preparation of plates

Since the preparations had to be observed using high NA microscope objectives, glass bottom petri dishes (35mm ϕ, 0.17 glass thickness) were used. Cortical neurons donot adhere to glass surfaces. However they do so efficiently to laminin coated surfaces. Laminin is a protein found in the extracellular matrix. Laminin binds to cell surface through integrin receptors on the cell membrane. This helps cells like neurons to adhere to laminin coated surfaces. Since laminin by itself does not adhere to glass surface, the glass surface is first treated with poly-L-ornithine. poly-L-ornithine adheres efficiently to glass surface and laminin adheres effectively to it. Neurons can subsequently be plated to such poly-L-ornithine/laminin substrates.

4.3.2 Dissecting out the cerebral cortex

First the embryos need to be dissected out of the female mouse. The mouse is anesthetized in chloroform and neutralized. Neutralization is done by breaking off the neck using a pen, that cuts of the spinal cord. The abdomen is cleaned using alcohol and the embryos together with the uterus are removed out by making an incision in the abdomen of the mouse. The embryos are collected in dissecting media (see appendix B for detailed protocol) in a petri plate. The individual embryos are removed out of the uterus. The head is separated from the rest of the body and placed in another petri plate with dissecting media and observed under a dissecting microscope. The head is spit in half and a

small portion of the cerebral cortex removed out of the embryo brain. This is collected in a tube with HBSS (Hank's Balanced Salt Solution).

4.3.3 Dissociating the neurons

The piece of cerebral cortex collected in HBSS is treated with trypsin and incubated at 37^0C in a water bath for about 12mins. Trypsin is a serine protease found in the digestive system which breaks down proteins. Trypsin helps to break down the proteins that bind the neurons together in the brain tissue. This is the first step in dissociating the neurons. Subsequently trypsin is inactivated by NHS (Normal Horse Serum). The resultant is centrifuged (800rpm, 4^0C, 5mins). Dissociating process is completed by tituration using a flame polished pasteur pipette. This results in dissociated individual neurons in a suspension.

4.3.4 Plating the cells in a culture dish

A small amount of the cell suspension is plated on the poly-ornithine/laminin culture dish with about 200μl of culture media (see appendix B), supplemented with B27 and N2. A small amount of purified recombinant NGF (nerve growth factor) (4ng/ml) is also added to the dish. The dishes are incubated for 18 hours in a 5% CO2, 95% humidity incubator at 37^0C. Before transportation about 2ml of culture media buffered with HEPES is added.

4.4 *C.elegans*

Caenorhabditis elegans is a free-living, transparent nematode (roundworm), which lives in temperate soil environments. A number of interesting features has made *C.elegans* a model organism in biology. These are:

- The *C.elegans* genome was fully sequenced in 1998 and considerable conservation of biological mechanisms across the animal kingdom is established. In addition its cell lineage has been fully established
- It is transparent and hence easy to observe under a microscope.
- Has a short life cycle (about 3 days), small size and very easy to maintain in large quantities.
- Self-fertilization in hermaphrodites allows homozygous worms to breed true and greatly facilitates the isolation and maintenance of mutant strains [143].
- Transferring of genetic traits can easily be done between strains by mating hermaphrodites with males.
- Even though it has only 1000 somatic cells, *C.elegans* is a highly differentiated animal. It therefore provides a tractable system for studies of metazoan cellular function, development and differentiation [143].

4.4.1 Basic *C.elegans* Biology

C.elegans predominantly feed on microbes and can easily be grown in the laboratory on agar plates with *E.coli* bacterial lawns. Adult *C.elegans* are predominantly hermaphroditic

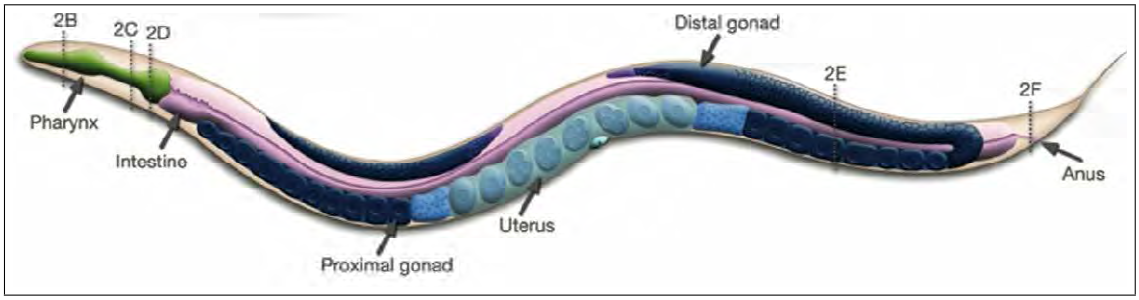

Figure 4.1: Schematic drawing of the anatomy of an adult *C.elegans* hermaphrodite worm. (Adapted from http://www.wormatlas.org/handbook/anatomyintro/anatomyintro.htm)

with males making up approx 0.1% of wild-type populations [143]. About 300 offspring are produced by self-fertilized hermaphrodites. When hermaphrodites mate with males about 1000 progeny are produced. The *C.elegans* life span is about 2-3 weeks under optimal laboratory conditions. It however has a rapid life cycle. At 25^0C, embryogenesis (the period from fertilization until hatching), occurs in 14 h [143]. Postembryonic development occurs in four larval stages (L1-L4) that last a total of about 35h [143]. The end of each larval stage is marked with a molt where a new, stage-specific cuticle is synthesized and the old one is shed. When food supply is scarce, larvae in the L2 stage progress to form dauers. Dauer larvae do not feed and have structural, metabolic, and behavioral adaptations that increase life span up to 10 times and aid in the dispersal of the animal to new habitats [143]. Once food becomes available, dauer larvae feed and continue development to the adult stage .

C.elegans has an unsegmented, cylindrical body shape that is tapered at the ends [144]. The body plan consists of an outer tube and an inner tube separated from each other by the pseudocoelomic space [144]. The outer tube (body wall) consists of cuticle, hypodermis, excretory system, neurons and muscles, and the inner tube, the pharynx, intestine and, in the adult, gonad [144]. Figure 4.1 shows some of the anatomical features of an adult hermaphrodite worm.

The body wall consists of tough collagenous cuticle secreted by the underlying hypeodermis, muscles, and nerves [143; 144]. The excretory pore, vulva and anus open to the outside through the cuticle. A fluid-filled body cavity or pseudocoel separates the body wall from internal organs. Body shape is maintained by hydrostatic pressure in the pseudocoel [143]. *C.elegans* feeds through a two-lobed pharynx which is nearly an autonomous organ with its own neuronal system, muscles, and epithelium [144]. The lumen of the pharynx is continuous with the lumen of the intestine and the pharynx passes ingested and ground food into the intestine via the intestinal pharyngeal valve [144]. The rectal valve that connects the gut to the rectum and anus excretes the intestinal contents [144]. The reproductive system in *C.elegans* hermaphrodites consists of somatic gonad, the germ line and the egg-laying apparatus. The gonad consists of two bilaterally symmetric, U-shaped gonad arms (ovaries) that are connected to a central uterus through spermatheca [144]. The germ cells go sequentially through the mitotic, meiotic prophase and diakinesis stages [144]. The nuclei acquire plasma membrane to form oocytes as they pass through the bend of the gonad arm (oviduct) [144]. The oocytes enlarge and mature as they move

more proximally. They fertilize with the sperm in spermatheca and the zygotes are stored in the uterus and laid outside thorough the vulva which protrudes at the ventral midline [144]. Male anatomy is similar to the hermaphrodite anatomy until the second larval stage. The male differs significantly in tissues of the posterior, which bears the male copulatory apparatus [144]. The muscle system of the male contains additional 41 sex-specific muscles. The reproductive system consists of a single armed gonad that opens to the exterior at the cloaca (anus) via a modified rectal epithelial chamber called the proctodeum [144].

4.4.2 *C.elegans* Muscle

There are two types of muscle in *C.elegans*: multiple sarcomere/obliquely striated (somatic) muscle and nonstriated muscle [144]. The muscle found most abundantly is the striated body wall muscles (95 cells) [143]. They are arranged in longitudinal bands along the body wall and are responsible for locomotion. Nonstriated muscles are associated with the pharynx (20 cells), intestine (2 cells), anal sphincter (1 cell), anal depressor (1 cell), the hermaphrodite uterus (8 cells), gonad sheath, and vulva (8 cells). These muscles are responsible for pharyngeal pumping, defecation, ovulation and fertilization, and egg laying [143]. Males have specialized nonstriated muscles (41 cells) that are located in the tail and function in mating. Figure 4.2 shows a schematic representation of body wall and enteric muscles.

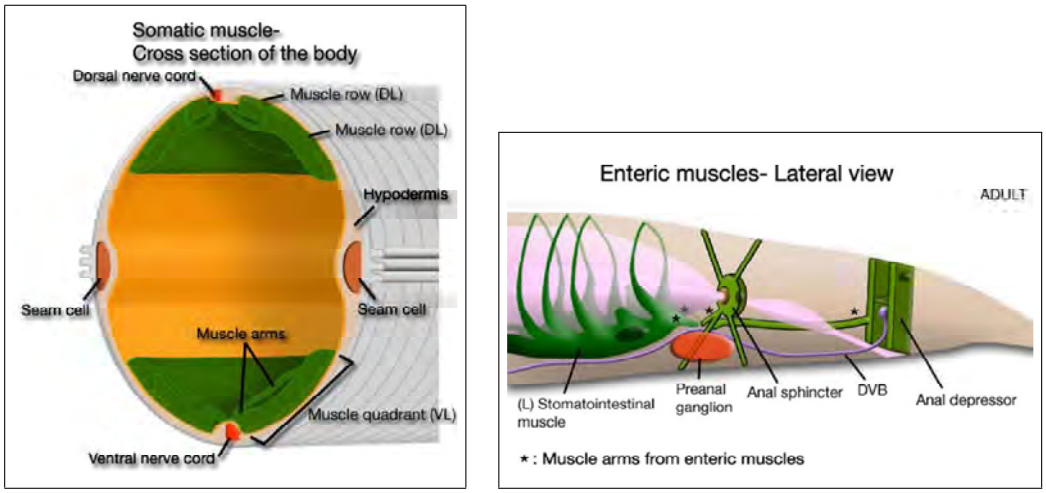

Figure 4.2: Schematic drawing showing somatic and enteric muscles of an adult *C.elegans* hermaphrodite worm. (Adapted from http://www.wormatlas.org/handbook/mesodermal.htm/musclepartI.htm)

The muscle is made of the fundamental unit called the sarcomere. Figure 4.3 shows the schematic representation of sarcomere. This is an ato-myosin complex, meaning it is made of actin and myosin. The actin filaments called the thin filaments slide into the myosin filaments (A band) called the think filaments. The region where actin slides into myosin is called the H zone. This sliding feature provides the sarcomere with the ability to contract. The region which has only actin is the I band and region which has only myosin is called the M line. The z discs are located at the ends of the sarcomere.

The striated muscle have multiple sarcomeres and contain evenly distributed attach-

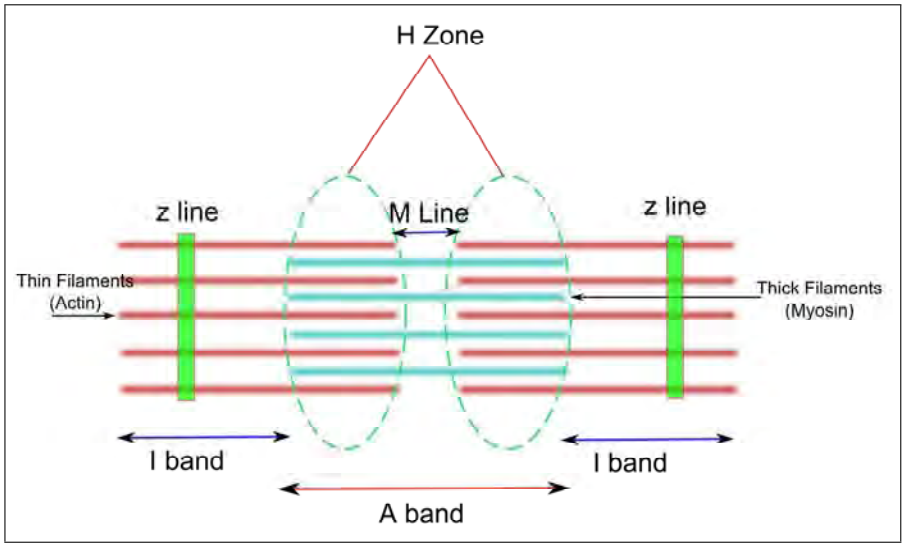

Figure 4.3: Schematic drawing of the sarcomere

ment points to the hypodermis and cuticle along their length cite [145]. The nonstriated muscles have focal attachment points at their ends. The pharyngeal pumping behavior of the pharyngeal muscle, gonadal sheath contractions, and defecation cycle involving body are controlled by intercellular Ca^{++} transients rather than excitation by neuronal transmission [145]. Nematode muscle cells extend processes to their target muscle cells which is unlike other organisms where neurons send processes to their target muscle cells.

In *C.elegans* there are 95 rhomboid-shaped striated body wall muscle cells. These cells are arranged as staggered pairs in four longitudinal bundles located in four quadrants [146]. These muscles help the worm in locomotion. A thin basal lamina separates these muscles from the underlying hypodermis and nervous cells [146]. Unlike vertebrate muscle which is cross striated and in register with adjacent sarcomeres, nematode muscle is obliquely striated and sarcomeres are offset from each other by more than a micron [146]. The observed A-I striations are at an angle of $5\text{-}7^0$ to the longitudinal axes of the filaments and the muscle cell, in comparison to 90^0 in vertebrate cross-striated muscle [146]. The smooth bending of the body without any kinking is thought to be a result of the oblique arrangement of the sarcomeres.

The non-straited muscle is quite different form the straited body wall muscles. The nematode nonstriated muscles have either one or a few well-structured sarcomeres or have myofilament networks that are less well organized [147]. The pharyngeal muscle, anal depressor muscle and vulval muscles contain only one sarcomere [147].

The pharynx muscle has eight distinct muscle divisions. Each of these divisions contain one to three muscle cells [147]. Each division except the most posterior one has threefold radial symmetry. The lumen in the pharynx is opened by the contraction of pharyngeal muscle cells [147]. There are a total of eight pharyngeal muscle ell layers (pm1-pm8). The first five pharyngeal muscle cell layers (pm1-5) have radially oriented filaments attach medially to the cuticle of the lumen and laterally to the pharyngeal basal lamina by hemidesmosomes [147]. pm6-pm8 form the grinder system of pharynx, help grind the

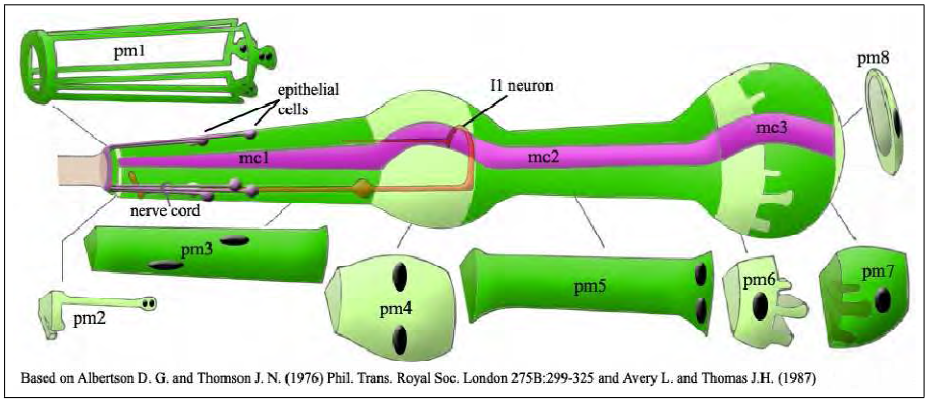

Figure 4.4: Schematic drawing of the pharyngeal muscles (From http://www.wormatlas.org/handbook/alimentary/alimentary1.htm)

ingested bacterial suspension. pm6 has three posterior projections that extend into pm7 and filaments are excluded from the middle one of these projections [147]. A longitudinal and radial component to the motion of the grinder teeth when it contracts is provided by the radially as well as longitudinally oriented filaments of the pm7 [147]. Similar to pm1-5, pm8 has radially oriented filaments that attach to the lumenal cuticle and the pharyngeal basal lamina at their ends [147]. All muscles except pm8 are innervated by pharyngeal motor neurons. pm8 does not receive any direct innervation from any of the motor neurons. Figure 4.4 depicts the schematic representation of pharyngeal muscles.

The cells of the ventral epidermis is connected to the surfaces of the intestinal cell by two sheet-like stomatointestinal muscle cells [147]. These muscles have few, longitudinally oriented filaments which are located in the ventral regions of the cells [147]. These cells have dorsally, thin, flat processes. These processes wrap around the posterior regions of the intestine and contain a few vertically oriented myofilaments which attach to the dorsal body wall by hemidesmosomes [147].

The anal muscles help in the defecation process. The anal sphincter muscle controls the rectal valve. This muscle has a single toroidal cell that contains a continuous ring of contractile filaments [147]. The anal sphincter muscle circles the intestine at its junction with the rectum. The anal depressor muscle widens the anal opening for defecation. This muscle is differently organized in males and hermaphrodites. In hermaphrodites it is a large, single sarcomere, H-shaped muscle that runs vertically between the dorsal wall of the rectum and the dorsal hypodermis [147]. In males, the anal depressor contractile apparatus detaches from the dorsal hypodermis and attaches to the dorsal spicule protractor during L4 molt, reorienting myofilaments to run anteroposteriorly in this muscle [147].

Some muscle cells are specific to the hermaphrodites. They have eight vulval muscle cells. These muscles control the vulval opening, which is used to eject the embryos form the uterus. These muscles have single srcomeres and exist in two sets of muscles (vm1 and vm2) that each contains 4 cells [147]. The single sarcomeres of vulval muscles stretch along the entire muscle length and attach to discrete zones in the body wall at one end and to the vulval epithelium and vulval cuticle at the other by hemidesmosomes at late L4 stage [147]. The hermaphrodites also have eight uterine muscle cells. The uterus is wrapped

around in each half by the distal set of two uterine muscle (um2) cells that form a full band [147]. Each of the proximal set of two muscles (um1), on the other hand, make a half band which wraps around the proximal uterus on the ventral side and attaches to it close to the vulva [147]. These muscles move the eggs though a squeezing action. Hermaphrodites also have 5 pairs of gonadal sheath cells. They are positioned along the proximal-distal axis of the gonad and cover the germ line tissue of each gonadal arm [147]. These sheath cells form a dense network by abundantly expressing actin and myosin. During ovulation, contraction of the proximal sheath pulls the dilated spermatheca over the most proximal oocyte and hence transfers this oocyte into the spermatheca for fertilization [147].

C. elegans males have 41 specialized nonstriated mating muscles. There are 15 diagonal muscle cells which contain 3 sarcomeres per cell. The longitudinal muscles have 10 cells with well structured sarcomeres that orient in tandem to the ventral body wall muscles [147]. There are 8 single sarcomered cells in the spicule protractor and retractor muscles. There are 2 gubernacular erectors and 2 gubernacular retractors, all of which are single sarcomered [147]. In addition there are also 4 oblique single sarcomered muscles [147].

4.4.3 *C.elegans* Nervous System

The nervous system of *C.elegans* consists of 358 cells in hermaphrodites and 473 cells in males. Of these 302 are neurons in hermaphrodites and 381 in males. There are 20 pharyngeal neurons that work independently of the 282 somatic neurons of the bodywall and hence the nervous system is divided into the pharyngeal and central nervous systems [148]. The pharyngeal neurons are connected to the CNS thorough two interneurons. The majority of the body neurons and synapses are brought together at the nerve ring in the head [148]. The ventral and dorsal nerve cords as well as the preanal ganglion in the tail forms the other regions of synaptic interaction [148].

The sensory neurons have specialized dendrites that are either embedded in the cuticle of the bodywall or protrude to the outside through openings in the cuticle. These neurons sense mechanical (by deformation of cuticle) or chemical signals [148]. The sensory functions involves chemotaxis, ordertaxis and touch response [148]. Some sensory neurons are not directly exposed to the outside but embedded deeper in the amphid sheath (eg: AWA, AWB and AWC neurons) [148]. The sensory neurons can be divided into chemosensors (eg: ADF, ASE, ASG, ASJ, PHA), odorant sensors (AWA, AWB and AWC), thremosensors (AFD), mechanosensors (eg: ADE, CEP, OLL, ALM, AVM, PVM), oxygen sensors (AQR,PQR and URX) amd proprioceptors (eg: ALN, PVD, AVG, I2, I3)

The motor neurons are divided into various classes. Motor neurons whose Nuero Muscular Junctions (NMJs) lie in the nerve ring and control the head muscles [148]. Motor neurons acting in the nerve ring and the ventral cord cells control the neck muscles. There are a number of neuronal cells along the length of the body that control bodywall muscles and hence locomotion. These cells (DA,DB,DD,VA,VB,VC,VD and AS) have their cell bodies in the ventral nerve cord.

The works reported in this thesis have quite extensively used a transgenic strain of *C.elegans* that expresses GFP in its DD and VD type motor neurons. The DD and VD type motor neurons which are 6 and 13 in number respectively, function as reciprocal inhibitors during sinusoidal movement of the worm and use GABA neurotransmitter for inhibitory action. DA, DB, DD and AS extend commissures to synapse with dorsal muscle cells [148]. The VA, VB, VD and VC neurons innervate ventral muscles. The DD neurons

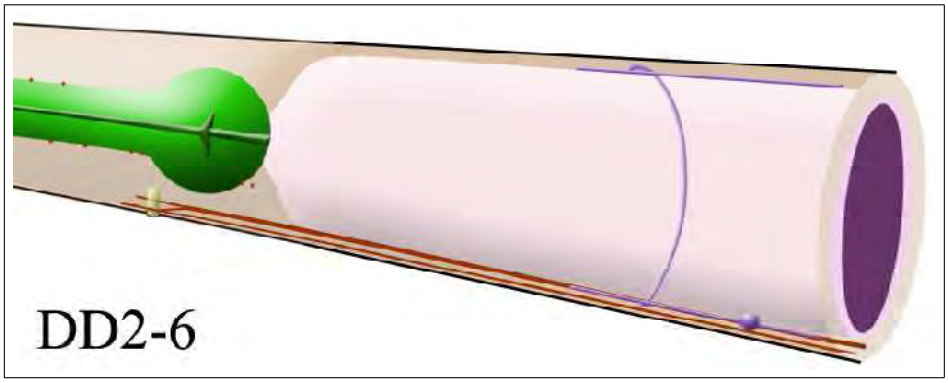

Figure 4.5: Schematic drawing of a typical DD type motor neuron. (Adapted from http://www.wormatlas.org/neurons.htm/DDn.htm)

send an axon to the dorsal nerve cord, while they receive inputs from other neurons through the ventral cord. The muscles in the dorsal side send muscle arms to the dorsal nerve cord to form NMJs and receive neuronal inputs from the DD type neurons. In most organisms the neuron sends branches to target muscles, whereas in *C.elegans* ventral cord neurons, the muscles receive inputs by sending arms to the nerve cords. Figure 4.5 shows the schematic of a typical DD type motor neuron. The VD neurons extend dendrite to the dorsal cord and receive inputs form it. The ventral side muscles send muscle arms to form NMJs with the ventral nerve cord to receive VD neuronal inputs.

The pharynx is controlled by five classes of motor neurons M1-M5 [148]. These are intrinsic to the pharynx and function as an autonomous unit. In males the tail has 41 specialized muscles for male mating behavior. These muscles are controlled by male specific motor neurons. The control of egg laying in hermaphrodites is done by control of the vulval muscles through the HSN and VC neurons. Defecation is controlled by the contraction of the posterior body under the control of AVL and DVB motor neurons. These neurons are believed to be triggered by a calcium signal origination in the posterior intestine [148].

There are also several classes of interneurons in *C.elegans*. These neurons receive information form some neurons, process this information and relay it to other neurons [148]. The most important among them are the command interneurons (AVA, AVB, AVD, and PVC). These interneurons act as intermediaries in locomotion by collecting inputs form the nerve ring and tail ganglia and relying the information to the ventral cord motor neurons [148]. The signals from many chemosensory neurons of the amphid class are first fed to the interneuons AIA and AIB, which sort these signals according to priority [148]. The temperature sensed by the AFD neuron is compared by the AIY and AIZ interneurons with a secondary signal to detect changes in temperature over time [148].

There are also several polymodal neurons that are multitasking in nature. The NSM neuron in the pharynx function as a motor neuron as well as a secretory cell. The MI neuron also in the pharynx multi tasks as motor neuron and interneuron [148]. The IL1 neuron in the head doubles as a mechano-sensor as well as motor neuron.

4.4.4 *C.elegans* Culture

C.elegans worms are grown in petri plates with Nematode Growth Media (NGM) with a agar base. The food for *C.elegans* is bacteria, usually the *E.coli* strain OP50. The bacterial suspension is spread over the NGM plates to form a bacterial lawn and the worms are let to crawl on these lawns. The lawn is limited to a certain region of the plate to facilitate easy observation and transfer of worms. The OP50 strain is auxotrophic for Uracil and hence grows only in Uracil supplemented environment like the NGM [149]. This helps prevent contamination. A starter culture of E. coli OP50 can be obtained from the *C.elegans* Genetics Center (CGC) or can be recovered from worm plates [149]. The starter culture is used to grow isolated colonies on a streak plate with rich medium such as LB agar [149]. A single colony is then used to inoculate a liquid media (liquid LB) to have a bacterial suspension. The streak plate and the liquid culture can be used for several months if stored at 4^0C [149]. For detailed protocol for making NGM and LB for bacterial cultures please see appendix C.

Plates of different sizes can be used for culturing *C.elegans*. Smaller plates (35mm diameter) can be used for matings or when using expensive drugs. Medium size plates (60 mm diameter) can be used for general strain maintenance, and larger plates (100 mm diameter) are useful for growing larger quantities of worms, such as for certain mutant screens [149]. The NGM agar medium can be poured manually or using a pump. The pump allows the same amount of media poured into each plate and avoids the need to refocus the microscope every time a new plate is placed under it [149]. Drugs or specific chemicals can be added the NGM before being poured. To seed the plates approximately 50μl and 100μl of bacterial culture (see appendix C) is poured respectively into small or medium and large culture plates and spread to form a lawn using a sterile spreader [149].

There are several methods to transfer worms to plates. The easiest way is chunking where a small piece of NGM is cut out using a sterile scalpel, from an old plate with worms crawling over it and placed in another fresh plate. The worms crawl out of the chunk and move into the bacterial lawn of the new plate. Individual worms can be picked out of a population using a worm pick. A worm picker can be made by mounting a 1-inch piece of 32 gauge platinum wire into either the tip of a Pasture pipette or in a bacteriological loop holder [149]. The picker should be sterilized between transfers by flaming it, to avoid contamination of stocks with microbes as well as cross contamination form other plates. The end of the wire, used for picking up worms, can be flattened slightly with a hammer and then filed with an emery cloth to remove sharp edges; sharp points can poke holes in the worms and kill them or make holes in the agar [149]. A bend flattened tip picker can be used like a hook to pull the worm up. This works well with worms in later stages of life cycle. A blob of bacterial suspension can be swiped out using the pick and and then used to gently touch the worm, whereby the worm sticks to the pick. The picked worm is slowly lowered into the new plate and gently touched on the surface. The worm then crawls out into the new plate.

C.elegans stocks can best be maintained between 16^0C and 25^0C, most typically at 20^0C. *C. elegans* grows 2.1 times faster at 25^0C than at 16^0C, and 1.3 times faster at 20^0C than at 16^0C [149]. If stocks gets contaminated, individual worms can be picked from regions not contaminated to new plates. If this does not work, adult worms with lot of embryos can be picked and put in a drop of sodium hypochlorite solution. The solution

kills everything except the embryo protected by the egg shell. The larvae that hatch out of these embryos after the hypochlorite has evaporated will be clean and can be transferred to new plates.

C. elegans can be frozen and stored indefinitely in liquid nitrogen (-196^{0}C) or in a cyro-freezer at -80^{0}C. Freshly starved young larvae (L1-L2 stage) survive freezing best. Well-fed animals, adults, eggs and dauers do not survive well [149]. Usually several plates of worms that have just exhausted *E.coli* and contain lots of L1-L2 stage larvae are used. The worms are washed with M9 solution, and collected in tubes and centrifuged. The pellet is collected and mixed with required quantity of freezing media which contains glycerol and transferred to 1.8ml cryotubes. The tubes are placed in a styrofoam box with slots to hold the tubes and placed in the cryo-freezer. The styrofoam makes sure that the worms are frozen gradually, without which they donot survive freezing. After about 12-24hrs the frozen cryo tubes are transferred to labeled boxes in the cryo-freezer. For detailed freezing protocol please refer to appendix C.

The recovery of *C. elegans* from stocks stored in liquid nitrogen is in the range of 35-45% of the total number of animals frozen. This number decreases only slightly after many years of storage in liquid nitrogen [149]. The recovery of stocks stored at -80C for many years (10) is not as high as liquid nitrogen, but worms can be safely stored this way for many years [149].

To recover worms from the frozen stock a small amount of the frozen stock is scooped out and placed on a fresh NGM plate with bacteria. As the scoop thaws some worms start to crawl out slowly. These worms are grown for two or three generations before being used for experiments.

Chapter 5

Optical Neuron Guidance

5.1 Overview

One of the standing goals of neuroscience is to look for ways to control neuron/axon growth. To externally induce guidance, several techniques have been employed including electric fields and use of focused light as optical tweezers. Ideally a mechanism that closely resembles the natural process of signaling the growth cone is desirable. Light can act as as putative agent to signal the growth cones and hence direct axonal growth. One of the primary aims of this thesis has been this study on the possible use of light to signal the growth cone in neurons. This chapter first describes, short duration observations of the filopodia, under the influence of weak NIR light sources. These light sources were placed at a small distance from the growth cone. Filopodia are the fundamental path finders in the growth cone of the developing neuron. Once it was established that the filopodia significantly orient themselves towards light of certain properties, long duration observations were made to study the effect of these distantly placed light sources on the whole axon. It was observed that the initial orientation of the filopodia subsequently leads to the whole axon growing towards the laser spot in a statistically significant number of cases if pulsed NIR laser light is used.

5.2 Introduction

The process of neuronal guidance is one of the most intricate and complex processes in neuroscience and has been target of attention from many different fields of study. One of the standing goals of neuroscience is to look for ways to control neuron/axon growth. This control could be the key to a potential formation of patterned neuronal networks and, even, neuron regeneration.

The natural process of axon guidance ensures error free networking of the complex nervous system. Growing axons have a highly motile structure called the growth cone [150–155]. During development the growth cone follows a precise pathway towards its target by scanning the extra-cellular matrix using the filopodia. This pathway is influenced by both signals in the extracellular matrix and intercellular communication. The sensory function of axons depends on extracellular cues which can be either attractive or repulsive. In this way, growth cone receptors sense the external cues and ultimately

guide axons towards the correct target [89; 90; 93]. These guidance cues fall into several classes of biomolecules [86; 156]. The progressing knowledge of these molecules has resulted in some of these being used externally to achieve control over neurite growth [129; 157]. Nevertheless, in view of the multifunctional characteristics of the phenomenon and the involved specific receptors (that activate complex intracellular signaling cascades in the growth cones), a successful guidance control is hard to achieve. As a result, precise and selective control of individual neurons can not be fully guaranteed. In the last twenty years there have been significant efforts in finding alternative guidance cues (other than biomolecules) that can manipulate and enhance the intrinsic natural growth process. Several methods have thus been suggested. These include the use of electric fields [105; 106], use of micropatterned substrate structures to restrict axonal growth to specified trajectories [158–160] or mechanical forces [132; 161].

In addition to all the aforementioned a number of works have highlighted the use of light as a potential tool to achieve control on axon guidance. For example laser photolysis of caged Ca^{2+} ions was used to induce a tropic turning of the axon [135]. In this work, the observed effect was attributed to an increase in the Ca^{2+} ion concentration in a localized region (laser focus) of the growth cone. Light's ability to impart mechanical forces has also been explored to achieve axon guidance in different cell lines. In these experiments a near infra-red continuous wave (CW) laser beam was made to fall on the edge of the growth cone to optically drag the neuron towards a certain course [137]. The main hypothesis attributed the guidance of the neurites to light's ability to gather actin monomers to provide nucleation sites for the actin polymerization which drives cellular growth. With this idea in mind, axonal guidance was also achieved using an asymmetric optical trap line profile to better direct the optical forces in a chosen direction [138]. In contrast to this, similar levels of axon growth were shown regardless of the direction of the intensity variation along the optical line trap [140]. In addition the attraction efficiency while guiding axons with laser light has been tested for different wavelengths [139]. Neurite outgrowth of PC12 cell lines has also been observed under LED illumination [162]. However this outgrowth only occurred at a specific wavelength (479nm). Notably, the underlying mechanisms responsible for the light-cell interactions described above, have not been fully understood or are not known.

Light-cell interactions, and its benefits in medical applications have been extensively reported. Near infrared (NIR) wavelengths causes an increase of oxidative metabolism of the cytochrome c oxidase (transmembrane protein complex found in mitochondria) due to an excitation of a chromophore. As a result, there is an enhancement of the mitochondria functionality and, therefore, of the cell metabolism in general. This is the basis for photobiomodulation therapy used in spinal cord nerve repair, wound healing [163] and applied also to promoting functionality of primary neurons [164]. Moreover, photo irradiation can generate significant biological effects such as cell proliferation, collagen synthesis and the release of growth factors from cells [165]. In addition, visible light has been shown to trigger calcium-dependent exocytosis in primary chicken telencephalic neurons, building up plasma membrane [166]. The opsin 3 found in these neurons were suggested to be the putative light receptor molecule responsible for this light-induced exocytosis. Nonretinal/nonpineal opsins have been studied as natural photoreceptors and their expression in deep brain neurons are well established [167].

Light has also been shown to act like a signaling agent to remotely communicate with

cells. 3T3 cells were shown to extend pseudopodia towards single microscopic infrared light sources at a distance [168–170]. The strongest responses were observed if the infrared light sources emitted light of wavelengths in the range of 800-900 nm intermittently at rates of 30-60 pulses per min. Independently of the explored responsible mechanism behind this cell response, light seems to work as a communication mechanism between cells implying cell sensitivity to these wavelengths.

Considering all the above mentioned studies it seemed very likely that light could induce similar signaling effects on neurons. We were hence prompt to further explore this possible signaling mechanism of light and its use to control the growth process of axons. Specifically, we intended to investigate how the growth cone and the axon in neurons from the cerebral cortex of mouse embryos, respond to distantly placed NIR light spot through the study of its guiding efficacy. For this a NIR laser beam was focused at some distance away from the growth cone of primary neuron cultures. Our initial studies on the filopodia pointed to their ability to orient themselves towards the direction of a laser spot placed at a distance from the growth cone only when femtosecond-pulsed regime was used. We subsequently explored how this initial influence of the distantly placed light on the filopodia translated onto the axon and modified its subsequent growth. Particularly axon's ability to grow towards distantly placed NIR laser spots was investigated under different temporal regimes: continuous wave (CW), chopped CW and femtosecond (FS) pulses. We observed significant axonal growth towards the laser spot equally in FS and chopped CW regimes. This steering effect on the axon, however, was not well evident when CW laser light (without pulsing) was utilized.

5.3 Cell Culture

OF1 embryos (Iffa Credo, France) were used. The mating day was considered embryonic day 0 (E0). After anesthesia of the dams, embryos were dissected out and collected in 0.1% phosphate-buffered saline (PBS) and 0.6% D-glucose. Low-density dissociated cultures were established from the cerebral cortex of CD1 mouse embryos at 15 days gestation (E15). The dissected tissue was trypsinised (0.05% trypsin for 9 or 15 minutes respectively at 37^0C) and dissociated by trituration. All neurons were plated on a poly-ornithine/laminin substratum in 35mm diameter tissue culture Petri dishes. The cerebral cortex neurons were grown on Neurobasal supplemented with 10% normal horse serum, L-glutamine, $NaHCO_3$, D-glucose and supplement B27 (all from Gibco Life Technologies). Purified recombinant NGF (4ng/ml) (Sigma) was added to the cultures at the time of plating. All neurons were grown for 18 hours in a 5% CO2, 95% humidity incubator at 37^0C.

5.4 Experimental Setup

The experimental setup was build around a commercial inverted microscope (Eclipse TE 2000-U, Nikon). The schematic of the experimental setup is shown in Figure 5.1. The neurons were imaged using brightfield illumination provided by the microscope, and intermediate 1.5 magnification factor and with a 60x, 1.4 NA planapochromatic oil immersion objective. The behavior of the neurons was time-lapse recorded (1 frame each 5 seconds) using a CCD camera (pixel size of 4.5μm x 4.5μm) attached to one of the output ports

of the microscope. A chamber with an automatic heat control system was built around the microscope to keep the neurons at 37^0C. A Ti:sapphire laser oscillator (Mira 900f, Coherent), operating either in CW, chopped CW or modelocked femtosecond (fs) pulse regime was coupled into the microscope through the back port. This was achieved using a pair of galvanometric mirrors (used to steer beam during the conventional laser scanning modality for nonlinear microscopy), conventional relay optics and a 45^0 hot mirror to direct the beam through the microscope objective and towards the sample plane. The microscope objective focused the input laser beam onto the sample plane. The position of the focused beam was set by steering the beam to a fixed position in the XY plane before the start of each experiment. Fluorescence from a plane fluorescent sample was used to draw up a calibration curve between pixel coordinates in the CCD camera images and the galvanometric voltage which controlled the laser spot position. The cells were loaded after this calibration procedure. The laser spot could then be placed on the desired location by a simple mouse click on the image of the sample plane using a control software (programmed in Labview).

The focal position of the laser beam spot was adjusted by varying the height of the objective lens. Once the beam spot position was set, this remained unchanged (axially and transversally) through out the whole experiment. The program draws a colored dot in the image indicating the position where the beam lies. During the experiment, the color of this dot changes depending on whether the laser shutter is open or closed. Neutral density filters were used to attenuate the beam average power (in both pulsed and CW) down to 3mW at the sample plane of the microscope. This yields 40pJ energy per pulse and an irradiation of 2.4mJ/cm^2. The measured pulse duration at the sample plane was 240fs, which implies a net group delay dispersion introduced by the microscope of D = $2{,}100\text{fs}^2$ [171]. With the above parameters, the calculated spot size was 0.72μm.

5.5 Observing the Filopodia

Filopodia are the fundamental sensors in the growth cones [89; 90; 93; 156] and any external signaling that could modify axon growth should first result in filopodia orienting themselves in the direction of the external signal. Hence, filopodia response to distantly placed NIR light sources was investigated first.

5.5.1 Procedure

The laser light beam spot was applied at a distance of 15μm or more from the closest filopodium and within a semi-space defined by an angle of $\pm 90^0$ measured from the orientation axis defined by the axon (see Figure 5.2). The laser spot was maintained stationary in the same position during the whole experiment. The position of the beam was decided at the beginning of the experiment and was maintained fixed during the whole observation period. In order to determine the effects of the laser spot at a distance on the filopodia the following procedure was followed. Individual neurons were recorded without any laser excitation for the first 20 minutes. This period was used as a reference for the filopodium natural behavior and is referred to as control or OFF period. After that, the laser shutter was opened for a second period of 20 minutes, referred to as laser period or ON period. For the ON period two different conditions were used: ultrashort pulses (femtosecond) and CW laser light. This procedure was applied to 40 neurons under the influence of ultrashort

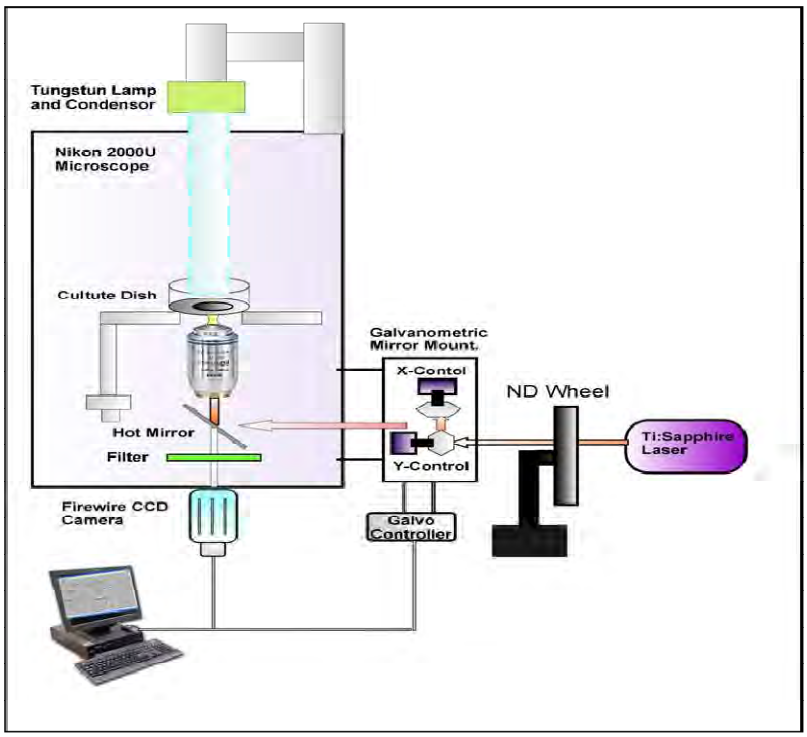

Figure 5.1: Schematic of the experimental setup used in optical neuron guidance experiments

pulses and 36 neurons under the influence of CW light. Each neuron was subjected only to one experiment involving 40 minutes (20 minutes OFF + 20 minutes ON) and only to one laser operating regime (FS or CW). Since the laser spot position was decided before the start of the experiment, during the OFF time when laser shutter is closed, the laser spot is a hypothetical spot whereas it is a real spot during the ON time when laser shutter is opened.

The control software was also used to capture the video-micrograph from the high resolution CCD camera at a rate of one frame each 5s for the whole experiment. The 76 neurons were analyzed in 8 different sessions (4 for the CW regime and 4 for the femtosecond one) where only one filopodium was analyzed per neuron. Each session was statistically treated as a different experiment to consider possible variations in the experimental conditions. None of the neurons were excited with more than one laser-period condition.

5.5.2 Preliminary filopodia analysis

The response of the filopodia of primary neuronal cultures were analyzed visually on a first hand basis. For this each recorded video with 20 minutes OFF period and subsequent 20 minutes ON period were observed visually. In a few cases with simple visual observation, it seemed that there could be a slightly favored orientation of the filopodia, towards the direction of the laser spot placed at a distance. This can be appreciated in Figure 5.3, where, in 5.3b when the laser is on, the filopodia seem more oriented towards the laser

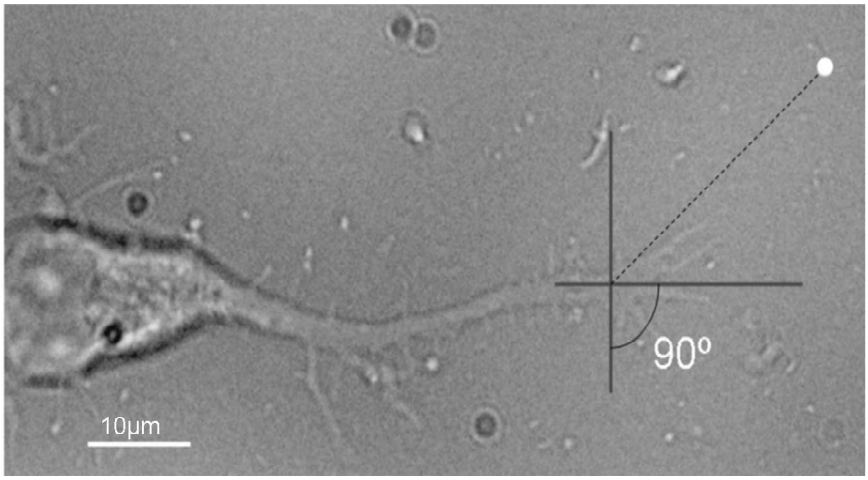

Figure 5.2: Snapshot of an axonal growth cone in which the position of the beam spot, represented by the white dot, is indicate in relationship to the orientation axis of the growth cone.

spot (blue spot) compared to 5.3a, when the laser is off. The green spot in 5.3a is the hypothetical spot showing the future position of the laser beam, when the laser beam would be on. The position of the laser spot as mentioned earlier is decided before the start of the experiment. This enables depiction of the hypothetical spot during the off period. Such observations (filopodia orienting towards the laser spot) were more frequent when the laser was operated in the femtosecond (fs) regime compared to the case when the laser was operated in the continuous wave regime (CW).

These visual observations gave an indication of the filopodia behavior towards distantly placed laser sources, however nothing was conclusive. Hence a method was devised to analyze the filopodia behavior in a systematic way. For this the video frames of each experiment were separately loaded in a Matlab program and the position of the tip of the filopodium was manually marked. The Matlab program displays the frames in the video

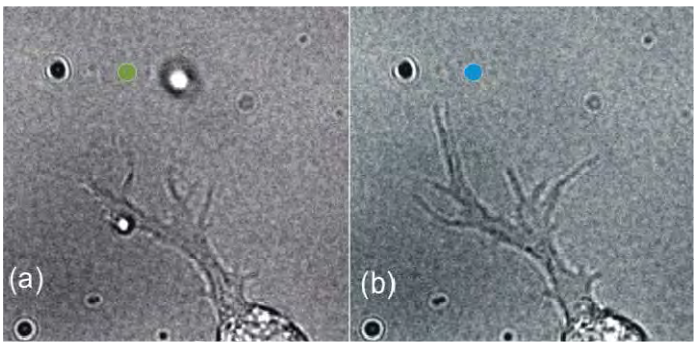

Figure 5.3: Snapshots of filopodia dynamics during the (a) OFF- and (b) ON- period where the blue dot represent the position of the focused beam (the green dot in (a) is placed only as a reference for the future beam position).

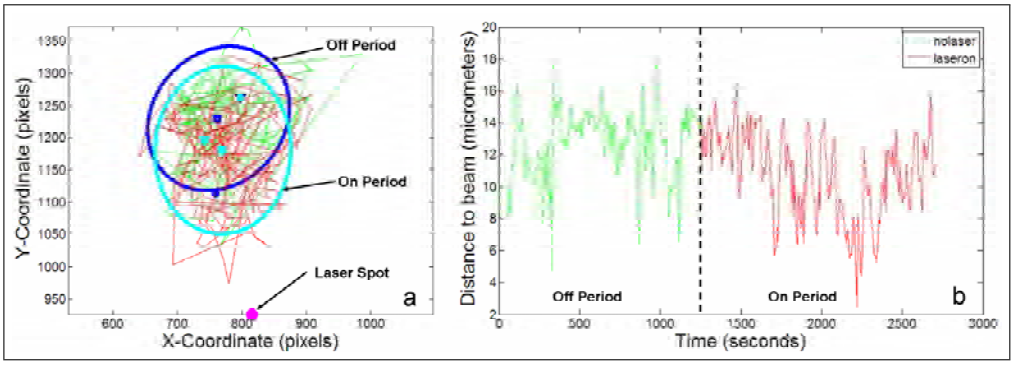

Figure 5.4: Filopodia dynamics a) Trajectory of filopodia in the x-y plane and b) distance of the filopodia to the laser spot as a function of time

one by one to the user and prompts the user to mark a point (by clicking the mouse pointer) corresponding to position of the tip of the filopodium under consideration. Once the user marks the point, the program records the marked position in terms of the pixel coordinate as a function of frame number. The program finally calibrates the frame number in terms of time and the captured pixel coordinate in terms of distance of that point form the laser beam position. The position of the laser spot is marked at the beginning of the execution of the program. The information is further used by the program to plot a graph of the distance of the filopodium to the laser spot in micrometers as a function of time and the trajectory of the observed filopodium in the x-y plane. The program also plots an ellipse in the trajectory graph, that best accommodates the whole trajectory of the filopodia during the OFF period and another ellipse that best accommodates the trajectory of the filopodia during the ON period. These ellipses helped make a rough estimation the orientation of the filopodia in general during the OFF and ON periods.

Figure 5.4 shows the dynamics of the filopodia in one of the observed neurons. Here, Figure 5.4a shows the trajectory of the filopodia in the x-y plane during the whole 40 minute observation period. The blue ellipse indicates the region in space where filopodia is when the laser is OFF (first 20 minutes) and the cyan ellipse indicates the region in space where filopodia is when laser is ON (second 20 minutes). Figure 5.4b shows the distance of the filopodia to the laser spot as a function of time. Here the green curve indicates the distance to the laser spot during the OFF period and the red curve indicates distance to the laser spot during the ON period. During the off period the laser spot as mentioned before is a hypothetical spot. The fact that the position of the laser spot is determined before the start of the experiment, facilitates assignment of the hypothetical spot position, where the laser spot would be placed during the ON period.

In the particular example shown in Figure 5.4, where the laser was operating in the FS regime, it can be easily observed that the cyan ellipse is more oriented towards the laser spot in the trajectory plot and the red curve in the distance graph is slightly shifted down. A down shifted curve in the distance graph implies proximity to the laser spot. This indicates a greater orientation of the filopodia towards the laser spot during the ON period compared to the OFF period. Such observations were increasingly frequent with the use of the laser in the femtosecond (fs) regime compared to the case when the laser is used in the continuous regime (CW), corroborating the visual observations of the videos

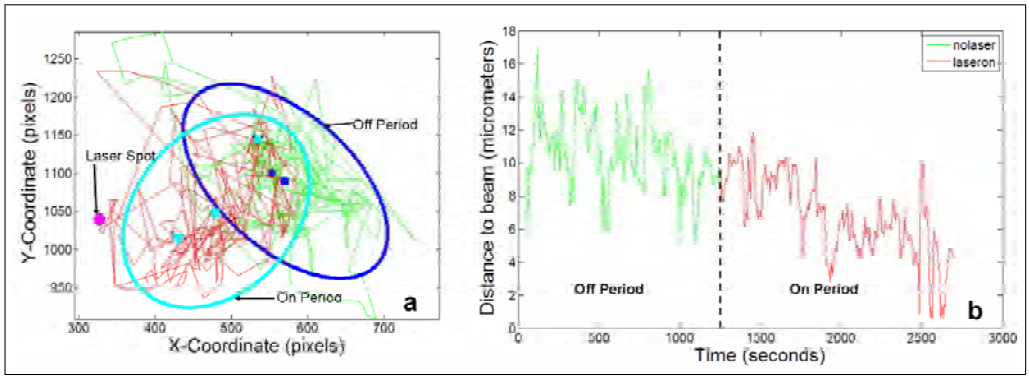

Figure 5.5: Filopodia dynamics of a case where the filopodia seem to touch the laser spot a) Trajectory of filopodia in the x-y plane and b) distance of the filopodia to the laser spot as a function of time

observed before.

There were also one or two cases where it seemed that not only where the filopodia orienting themselves towards the laser spot but also moving close enough so as to touch the spot. The filopodia dynamics of one such case is shown in Figure 5.5.

5.5.3 Detailed Filopodia analysis

Even though the preliminary filopoida analysis were increasingly pointing to the possibility of filopodia orienting themselves towards the direction of the laser spot when laser was operating in the femtosecond regime, it was difficult to fully ascertain, if this was just a matter of chance considering the highly stochastic nature of filopodia motion. Hence it was evident that a more detailed analysis methodology was required that obviated subjective decisions in determining if the laser beam exerts any influence on the behavior (displacement) of the filopodia (i.e., a tendency to orient towards or away from the beam).

A statistical approach was hence designed with the aim to distinguish between standard (normal) behavior and changes induced by an external stimulus. In this framework, two types of movements (displacements) can be defined. Ordinary movements are those displacements of the filopodia that are comprised within the standard deviation of such displacement. Analogously, extraordinary movements are those displacements beyond this standard deviation. Following this criteria, any external stimuli, including laser illumination, are assumed to be translated as an increment in the displacements beyond the standard deviation.

Taking as coordinate origin the beam position, the filopodium position p_f(n) is obtained at each video frame n (that is related to time). This allowed us to calculate the filopodium average position $\vec{P}_f$, its displacement p_f(n) with respect the average position resulting in a mean displacement m_f, and its standard deviation σ_f. These parameters were found considering the filopodium movements during both the OFF and ON periods. Figure 5.6 shows a typical example of the displacement followed by one filopodium, its average position and the region defined by the standard deviation (black circle). After that, our procedure is simply based on recording, as a function of the frame number n, the distance to the average position, P_f, and direction of these extraordinary displace-

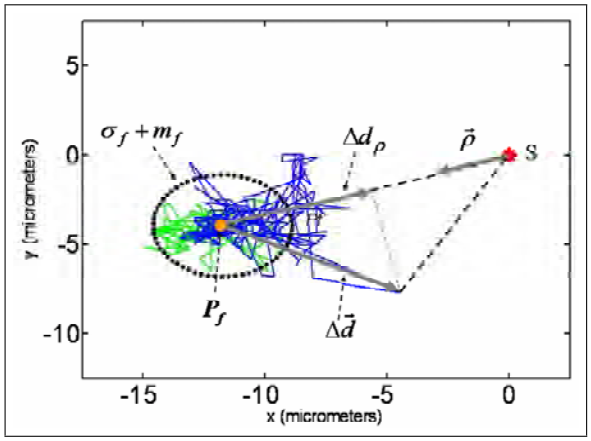

Figure 5.6: Recorded trajectory of a filopodium during the control-(*dashed green trace*) and femtosecond laser-(*blue trace*) periods. P_f is the filopodium average position, m_f is the average displacement and σ_f the standard deviation (defined by the *circle*). S is the position of the static beam. $\vec{\rho}$ is the unitary polar vector and $\triangle d_\rho$ the radial component for the extraordinary displacement vector $\triangle\vec{d}$

ments, i.e., those with $p_f(n) > \sigma_f$. These extraordinary displacements can be written in the vectorial form as $\triangle\vec{d}(n)$. This piece of information is then used to determine changes in activity and the influence of the laser illumination to induce a distal/proximal behavior on a particular filopodium.

We start with the measurement of the filopodium activity before and during laser illumination. We can assume that a higher number of extraordinary displacements during laser illumination, implying an increase in the filopodium movements, means an increment in the activity. On the other hand, a decrease in the number of extraordinary displacements would result in a decrease in the activity. Therefore the change in activity can be measured by taking the ratio of the extraordinary displacements in the ON period with respect to the OFF period:

$$\Gamma = \frac{\Sigma_{n\varepsilon ON} \mid \triangle\vec{d}(n) \mid}{\Sigma_{n\varepsilon OFF} \mid \triangle\vec{d}(n) \mid} \tag{5.1}$$

Note that zero change in the activity will give a coefficient with a value close to unity ($\Gamma \approx 1$). Within this framework, inactive neurons were those that had an activity one order of magnitude smaller ($\Gamma < 1$) than those with zero change in activity.

The next step in our procedure was to determine if a particular filopodium had a proximal or distal behavior, i.e., a clear tendency to move in the direction of the beam spot or away from it. Note that we took as coordinate origin the beam position. Therefore, in polar coordinates, the ρ component of an extraordinary displacement, i.e., $\triangle d_p$ indicates any movement in the direction of the beam. In this way, $\triangle d_p < 0$ indicates displacements towards the beam and $\triangle d_p > 0$ indicates displacements away from the beam.

Taking this into account, we can determine whether an individual filopodium has a net distal or proximal behavior during the ON or OFF period by defining a proximal

parameter as:

$$\Omega^{-}_{period} = \sum_{n\varepsilon period} \mid \triangle\vec{d}_p(n) \mid \Longrightarrow (for \triangle d_p < 0) \tag{5.2}$$

This parameter gives what is the total extraordinary displacement towards the beam. In the same way, the total displacement away from the beam is given by a distal parameter defined as:

$$\Omega^{+}_{period} = \sum_{n\varepsilon period} \triangle\vec{d}_p(n) \Longrightarrow (for \triangle d_p > 0) \tag{5.3}$$

By comparing the proximal and distal parameters, it is possible to estimate the tendency of a filopodium to move in a particular direction. For example, $\Omega^{-}_{OFF}/\Omega^{+}_{OFF} > 1$ indicates a clear tendency of the filopodium to move towards the beam position before the laser is switched on (during the OFF period). Similarly $\Omega^{-}_{OFF}/\Omega^{+}_{OFF} < 1$ indicates a net distal tendency of the filopodium in the same period. Similarly, $\Omega^{-}_{ON}/\Omega^{+}_{ON} > 1$ and $\Omega^{-}_{ON}/\Omega^{+}_{ON} < 1$ would correspond respectively to a proximal or a distal behavior in the ON period. Taking this into account, an ideal example of attraction would be a filopodia with an initial distal behavior $\Omega^{-}_{OFF}/\Omega^{+}_{OFF} < 1$ that switches to proximal behavior during laser illumination $\Omega^{-}_{ON}/\Omega^{+}_{ON} > 1$.

5.5.4 Results of filopodia analysis

Each individual neuron was analyzed using the filopodia analysis described in the previous section. We first calculated the change in activity (Γ) for the control, CW and femtosecond cases. We found that the number of neurons of a given Γ was similar, independently of the regime used. This can be seen in Figure 5.7 where the frequency distribution of Γ is shown.

This suggests that the presence of light (in either pulsed or CW regimes) at the employed average intensities, seems not to negatively affect the amount of activity of the filopodia. The results also showed that in all the sessions, $< 20\%$ of the neurons (see Table 5.1) exhibited a significant decrease in the activity ($\Gamma < 0.1$). This observed decrease in activity might be attributed to internal neuron dynamics: neuron weakness, exhaustion of biological material needed for growth, or even the neuron undergoing apoptosis. Thus, in what follows, we have excluded from our analysis all those cases which has an activity parameter $\Gamma < 0.1$.

Table 5.1: Percentage of inactive neurons

	(Number of neurons)	(Percentage of neurons with $\Gamma < 0.1$)
Femtosecond	40	12.5
Continous Wave	36	19.4
Control	76	17.1

We now focus our attention on understanding the global tendency of the filopodia to move in the direction of the beam or away from it. This was done by calculating the percentage of filopodia showing a proximal behavior, in both the OFF and ON periods (note that the distal behavior is the complementary of the proximal). The results are summarized in Table 5.2.

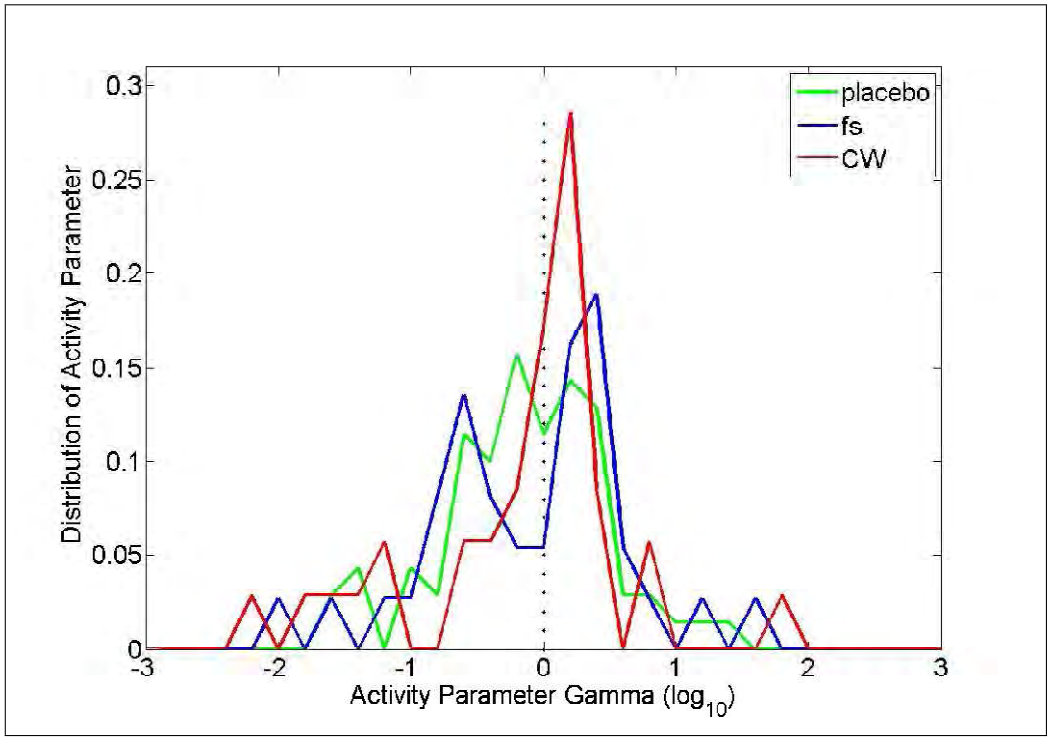

Figure 5.7: Change of activity (Γ) of the different filopodia for the control (*green*), CW (*red*) and fs (*blue*) regimes

Table 5.2: Percentage of proximal behavior: $\Omega^{-}_{ON}/\Omega^{+}_{ON} > 1$

Period	Control(%)	Cases CW(%)	Cases fs(%)
OFF	56	57	63
ON	61	65	88

It should be noted that, in an ideal control situation, the population distribution should be equally spread (50%) between the distal and proximal behavior (for both the OFF and ON periods as no laser is used). This is because in a random process like filopoida motion, there is equal probability that the tip of the filopodia can move towards or away from a particular point. However, the number of cases with proximal behavior is larger than the distal situation in the control case. This can be explained taking into account that the natural growth direction of the axon normally will occur within the semi-space in front of the growth cone, where the laser beam (in this case virtual) is located. This natural proximal behavior offset is also observed during the OFF period for both the CW and femtosecond illumination. From these results we obtained the probability of a filopodium to show a natural proximal behavior as 59± 4%, among all observed cases. When using CW illumination, 65% of the filopodia showed a proximal behavior. This falls very close to the calculated natural proximal probability, suggesting that the effect of CW illumination, if any, is very small.

The situation drastically changes when using femtosecond illumination. Here the prox-

imal behavior increased to 88% of the cases, clearly outside the calculated natural proximal probability. This shows that the femtosecond laser illumination is inducing a clear attraction effect on the filopodia.

The significance obtained by computing the binomial test between the pulsed case and the control or the CW cases is α <0.01. This clearly shows that there is a statistical difference between the presence of the femtosecond laser spot and the use of a CW spot.

To confirm this result and check the feasibility of the statistical method used, we averaged the filopodia displacement p_f(n) over all the analyzed neurons under femtosecond and CW laser light conditions separately. Figure 5.8 shows the obtained results. The vertical dividing line (at 20 min) in figures 5.8a and 5.8c shows the transition from the OFF to the ON-periods. To obtain an even better understanding we also computed the displacement frequency distribution (see Figures 5.8b and 5.8d) corresponding to Figures 5.8a and 5.8c, respectively. It can be observed that, for the pulsed femtosecond regime (Figure 5.8a), the average position of the filopodia is clearly displaced towards the beam. This also appears as a downward shift of the blue curve indicating the frequency distribution for femtosecond laser period when compared to the OFF period indicated by the green curve.

During the OFF period the mean distance of the filopodia to the laser spot was 15μm with a standard deviation of 0.8μm. Analogously, the mean distance of the filopodia to the beam during the femtosecond laser-period was 12μm with a similar standard deviation (0.9μm). This analysis confirms that the pulsed laser has induced a measurable filopodia attraction towards the beam. In contrast, the results with the CW case in figure 5.8c and d do not show such average displacement of filopodia during the CW laser-period. Here, in both OFF and ON- periods, the filopodia mean position remains close to 15μm with identical standard deviation (0.8μm), resulting in an overlapped area in the displacement frequency distribution shown in figure 5.8d and an almost identical mean position. This clearly demonstrates that the population keeps behaving similarly in both periods and CW light does not induce any measurable effect on the filopodia behavior.

5.5.5 Inferences from observing the filopodia

The experiments done on observing the filopodia, demonstrated the capability of ultrashort pulsed lasers to induce a measurable effect on the filopodia of primary neuronal cell cultures. The methodology was based on placing the beam spot at some distance from the axonal growth cone and on using low average powers of 3mW to avoid any tweezing or heating effects. The filopodia activity could be convincingly and effectively assessed by analyzing its random displacement, showing first that laser light used under our experimental conditions, does not induce any negative effect on our samples. This was shown for three situations with different stimuli (CW, femtosecond and control conditions).

After rejecting inactive neurons, it was also shown that filopodia are in fact attracted by distant, stationary, focused, ultrashort laser pulses. Under the same conditions, the CW light produced no clear effect on the filopodia showing a similar behavior compared to the control situation. These results were obtained using a methodology based on filopodia movements and by analyzing those displacements beyond the standard deviation. These results were further confirmed by analyzing the average displacement behavior of all the experimented cases.

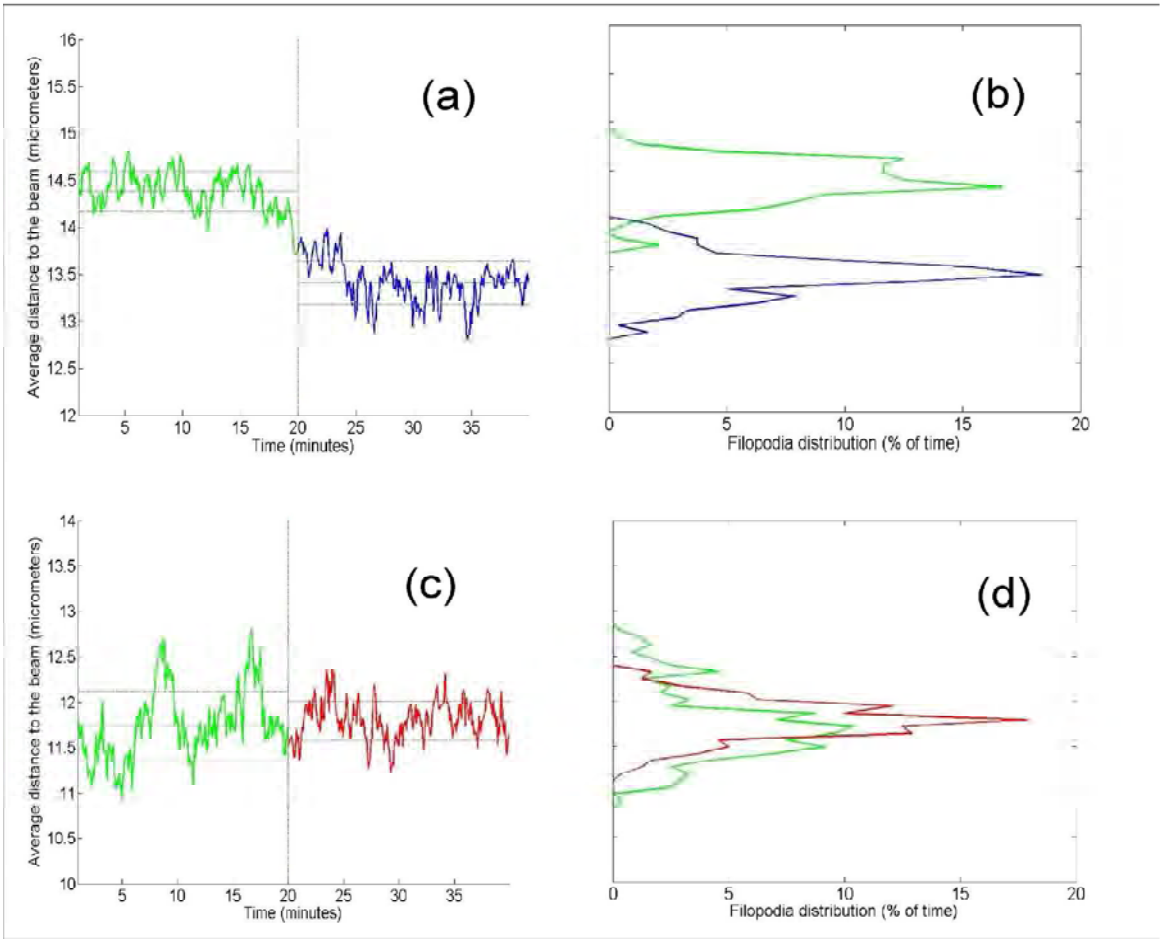

Figure 5.8: a,c) The displacement of filopodia in the beam direction averaged over all the observed cases during the laser and control periods for pulsed and CW cases respectively. b,d) The displacement frequency distribution of the average displacement of Figures a and c, respectively. In the pulsed regime, a strong orientation towards the beam can be observed. This behavior is not evident for the CW case at the same average power. Control (*green*), pulsed(*blue*), CW (*red*)

5.6 Observing the Axonal Growth

Once it was established that filopodia significantly orient themselves to the presence of pulsed femtosecond light spot placed at a short distance from the growth cone, it was left to analyze how this effect would manifest onto the axon and modulate its growth. To study this, a second set of experiments were preformed. The experimental setup, cell cultures and experimental procedure were exactly as in the first set of experiments observing the filopoida. Each of these experiments were however carried out for a much longer duration (3hrs) compared to the previous, since the axon dynamics are much slower than the filopodia dynamics [89; 90; 93; 156] . Here again a 800nm, 3mW average power (on the sample plane) light spot was placed at a distance between 10-20μm from the

growth cone.

70 different neurons were recorded under the influence of a laser focused spot placed in front of the growth cone and at a certain angle (within $\pm 90^0$) measured from the orientation axis defined by the axon. As before the position of the beam was decided at the beginning of the experiment and was maintained fixed during the whole observation period. Three different conditions of the beam where used: i) CW (22 neurons), ii) FS (37 neurons) and iii) chopped CW (26 neurons). In addition a control or sham situation (12 neurons) with no laser was used. None of the neurons were used for more than one recording experiment at a time. Each of the experiment had a maximum duration of three hours.

5.6.1 Axon's response to the use of CW and FS laser regimes

The behavior of 70 different neurons was recorded under the influence of a focused laser light spot which was also maintained fixed during the whole experiment in front of the growth cone. In these new set of experiments (observing axons), three different conditions of the laser beam were used: i) CW (22 neurons), ii) FS (37 neurons) and iii) Control (12 neurons). For the control (sham condition) no laser was used. None of the neurons were used for more than one recording experiment at a time. Each of the experiment had a maximum duration of three hours; time deemed sufficient enough for axons to grow towards the distant spot. Experiments were deemed successful only if the axon grew towards the beam spot and at least one of the filopodium touched the spot.

After analyzing all the cases, it was found that the direction of growth of axons were influenced by the type of light used in the focal spot. Firstly, the sham (control) experiments resulted in 8.3% of the neurons arriving to the predefined hypothetical position of the beam. In the case in which a CW laser was used, this percentage increased up to 13.6%. This situation changed considerably when FS pulses were used, where 45.9% of the axons moved towards the beam. While using the pulsed femtosecond light, once a filopodium was in the vicinity of the beam spot, it remained there until touching the beam spot. Upon contact, the filopodium showed some retraction followed by repeated advances towards the beam. There were few cases where the whole growth cone would eventually get trapped in the laser spot. Figure 5.9 shows an example of an axon being attracted towards a FS beam spot. There were also cases where the axon turned significantly in order to reach the laser spot. One such example is shown in figure 5.10.

5.6.2 Response of axon to chopped CW laser illumination

Once it was observed that pulsed femtosecond light at a distance could attract neuronal axons towards itself, it was left to establish if this effect was due to the very high peak powers provided by the femtosecond light or merely due to the pulsed nature of the source. To verify this, a new set of experiments were carried out with chopped CW light (20 Hz chopping frequency). This would provide a pulsed character to the beam spot but without the high peak powers characteristic of FS pulses. As in all previous cases an 800nm, 3mW average power (on the sample plane) light spot was placed at a distance between 10-20μm from the growth cone. None of the neurons were used for more than one recording experiment at a time and each of the experiment had a maximum duration of three hours.

A total of 26 neurons were observed in this regime. Interestingly, 46.1% of neurons had their axons growing towards the chopped CW beam spot. This percentage is very similar

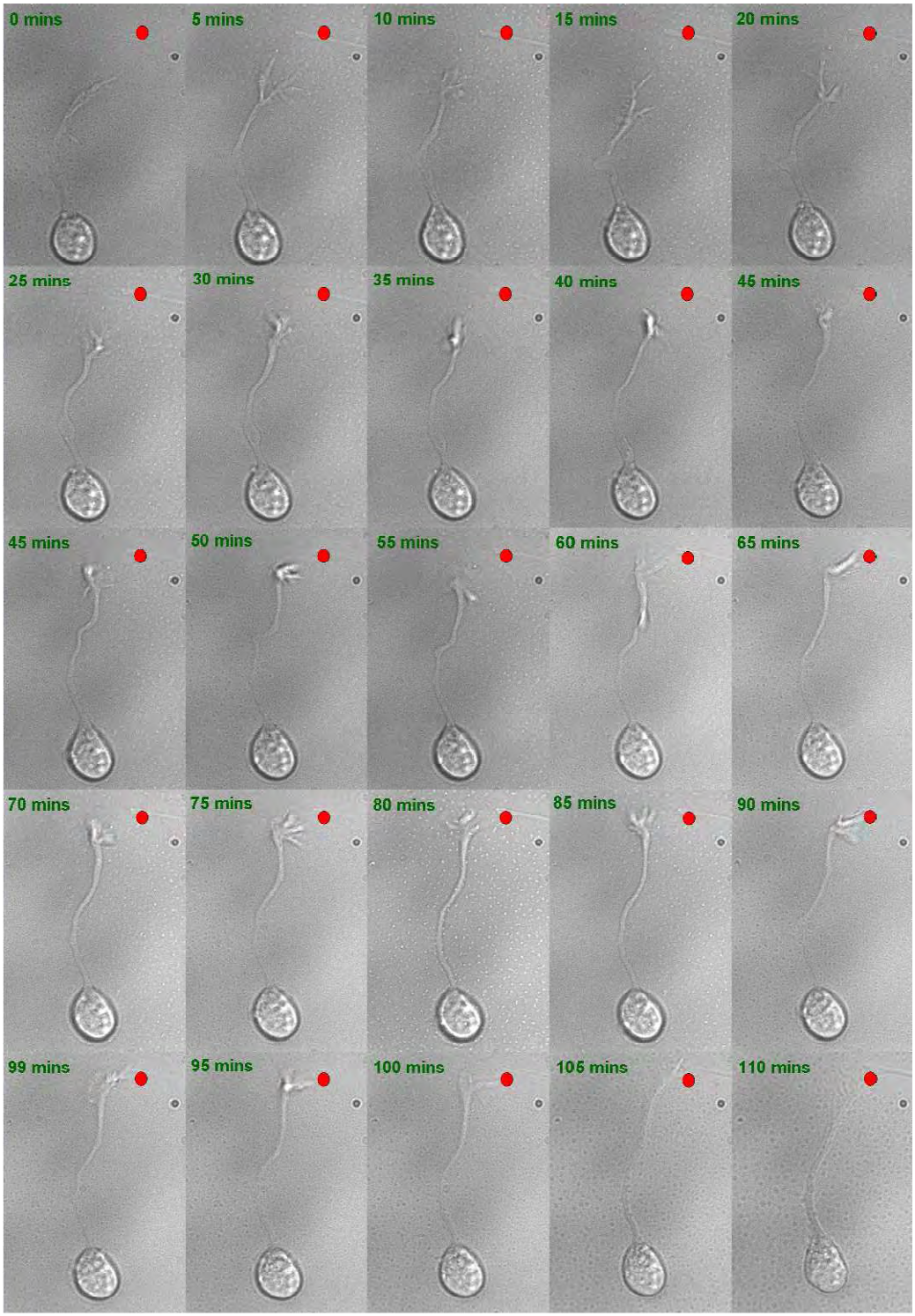

Figure 5.9: Example of an axon being attracted towards the FS beam spot. The red spot indicates the position of the laser spot (FS regime)

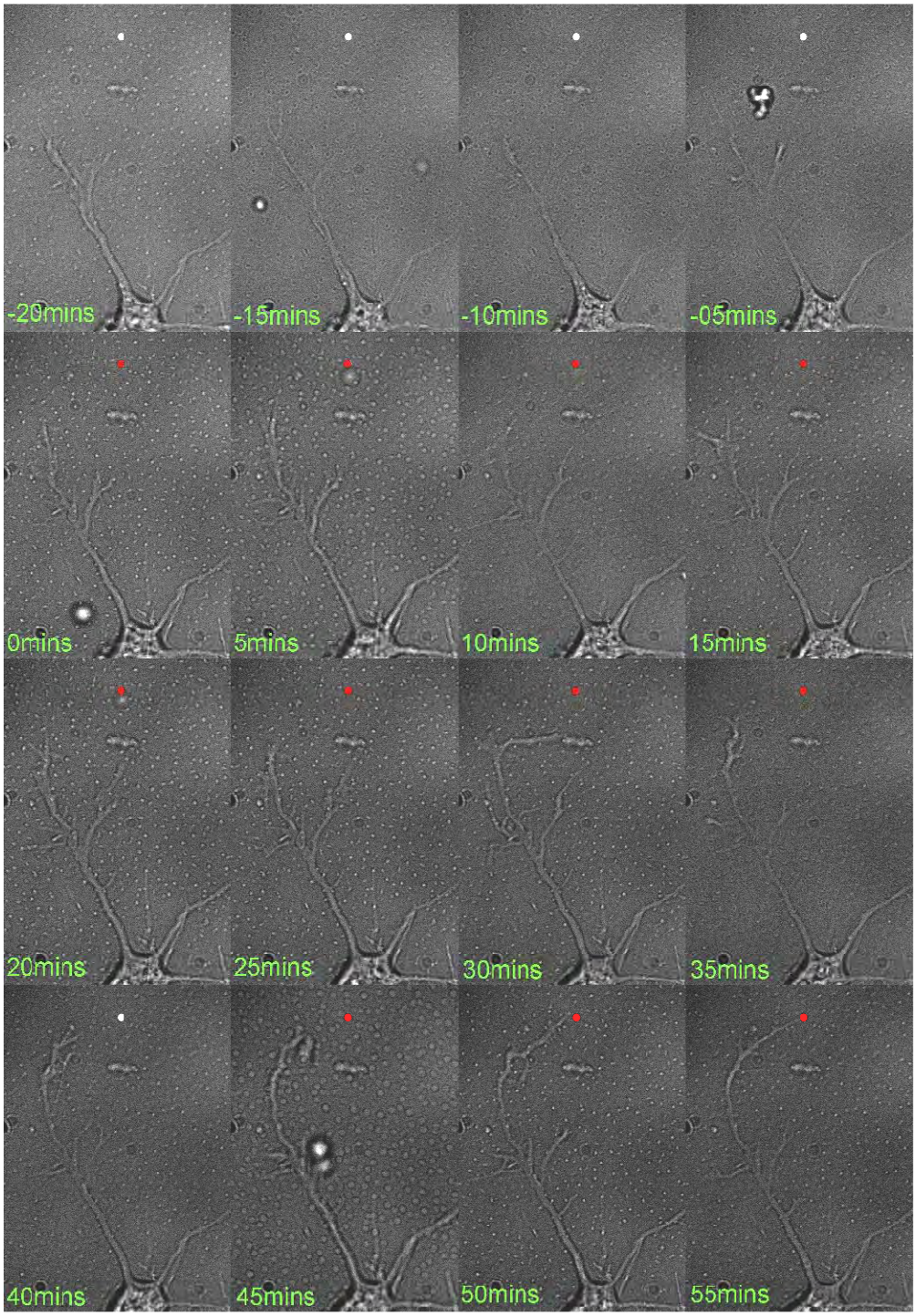

Figure 5.10: Example of an axon turning significantly to reach the distantly placed femtosecond light spot. The first 20 minutes the laser is off and the white dot indicates the hypothetical laser spot (future position of the laser spot). The red dot in the subsequent images shows the actual position of the laser spot.

to the case where femtosecond light was used. As seen in the case with femtosecond pulses once a filopodium was in the vicinity of the beam spot, it remained there until contacting with the beam spot. Upon contact, the filopodium showed some retraction followed by repeated advances towards the beam. There were again few cases where the whole growth cone would eventually get trapped in the laser spot.

The results of all the experimented cases on axons are summarized in Table 5.3

Table 5.3: Summary of experiment with axons.

Condition	N	Attracted	Attracted(%)	Non-Attracted	Non-Attracted(%)
Sham	12	1	8.3	11	91.7
CW	22	3	13.6	19	82.4
Chopped CW	26	12	46.1	14	53.9
Fs	35	17	45.7	20	54.3

5.6.3 Statistical Analysis

In order to evaluate the significance of our findings on axon's responses an exact binomial test was utilized. Here, the successful attraction frequency of the sham experiment is compared with the other three laser regimes: CW, FS and Chopped CW. Table 5.4 shows that there is no significant difference between sham and CW illumination. On the contrary, when compared with the sham experiment, pulsed excitations, i.e., Chopped CW and FS, are significantly different indicating that pulsed light produces a clear influence (in the form of attraction towards the pulsed laser beam spot) on the axonal growth.

Table 5.4: Results of the exact Binomial test.

Condition	Attracted	N	Mean and Standard Error	Significance of the exact Binomial Test(%)
Sham	1	12	0.08±0.08	
CW	3	22	0.13±0.07	0.424
Chopped CW	12	26	0.46±0.10	$4x10^{-7}$(<0.01)
Fs	17	35	0.46±0.08	10^{-9}(<0.01)

5.7 Discussion

The aim of this work was to examine the possible role of light in inducing signaling effects on the growth cone and, subsequently, on the whole axon of cortical neurons. Since the filopodia are the fundamental sensors in the growth cone, their response were analyzed first under short duration experiments and it was observed that they orient significantly towards the direction of distantly placed pulsed femtosecond laser spot. Other works utilizing light to induce mechanical forces to direct axonal growth have observed similar

orientation of filopodia in the direction of optical force prior to growth of axon in that direction [137; 140]. Therefore, such orientation of filopodia seems to be the principle indicator of the most probable direction in which the axon would grow.

Once the orientation of filopodia strongly suggested the possibility of axon growth in the direction of the pulsed laser spot a set of experiments were carried to determine the ability of pulsed femtosecond light to attract axons toward itself. Cortical axons in-vitro demonstrate great variability in growth rates but typically they could be expected to grow at a rate of few μm/hr. Hence the experimental duration for the second set of experiments were chosen to be 3 hours. This duration was deemed enough for the axon to grow towards the laser spot (placed typically at a distance between 10μm and 20μm), if the distantly placed laser spot was capable of inducing any significant influence. The results of these experiments demonstrated that a significantly large percentage (45.9%) of the axons were moving towards the beam. This is in contrast to the 13% and 8% of the cases for CW and sham cases respectively.

The question left to be answered was if the high intensity of the femtosecond pulses were inducing the attraction effect or if it was something related only to the pulsed nature of the source (and therefore, unrelated to the intensity). To investigate this, a third set of experiments were carried out with chopped CW light that would impart pulsed nature to the beam spot but without inducing any high intensity effects. The experimental conditions including the average power were maintained as in the previous experiments. Interestingly, the obtained results here were almost exactly the same as when FS pulses were used.

In experiments with pulsed light (chopped CW or FS), approximately 45% of the axons were arriving to a defined point (laser spot) within a cone of $\pm 90^0$ in front of the axon. This percentage may initially seem rather low. A rough estimate performed by considering the solid angle of the beam spot observed from the growth cone, gives an angle of less than 10^0 in all the studied cases. When compared with the considered 180^0 in front of the axon this result in a probability of 5.5%. Hence the probability that an axon would arrive randomly to specified distant position is only 5.5%. This is within the standard error of the sham situation given by the binomial test and also is suggesting that the CW laser spot seems not to make any major influence on the neurons. Moreover, the percentage of attracted axons when pulsed illumination is used are promising compared to those performed previously with pseudopodia of 3T3 cells where 25% of cells extend pseudopodia to distantly placed pulsating infrared sources compared to 4$\pm$2% in the control case [168]. The aforementioned arguments are strongly corroborated by the statistical analysis described before which attributes a strong influence when using pulsed NIR light (chopped CW and femtosecond). This indicates that the use of chopped CW or FS light exerts a strong influence on the trajectory of the axons by attracting them.

The question of what would be causing these effects needs still to be answered. Even though a definite answer seems elusive at this point and finding the exact reasons behind this effect out of scope of this work, it seems very likely that this effect is related to the pulsed nature of NIR light used since the effect is equally prominent when using chopped CW light and pulsed femtosecond light but not while using non-modulated CW light. The low average powers used in the experiment discard any thermal effect as origin. It has been reported that a 15mW CW laser at 780nm produced negligible heating effects at a distance of 5μm away from the focal spot [139]. An average power of 3mW at a distance

of more than 10μm as used in this work hence should not be generating any heating effect significant enough to affect axonal growth. In addition, the lack of appreciable attraction in non-pulsed CW definitively discards any thermal effect as origin.

It has been suggested by previous works that it seems very likely that cells communicate among themselves using infrared light. BHK cells separated by a thin glass window oriented themselves with respect to each other on opposite sides of the glass window when placed in the dark. This effect however was not observed when the glass slide was coated with IR blocking film. It was hypothesized that cells could communicate among themselves using NIR light, attributing some sort of rudimentary cellular vision [172].

It has also been observed that 3T3 cells fail to extend pseudopodia towards distant sources of constant intensity while they do so towards pulsating NIR sources. Taking into account also the previous argument it was hence postulated that external NIR light sources create a cross talk in the intracellular communication using NIR, and that pulsation helped the cells to distinguish the light sources form the constant thermal background radiation of their normal environment in a similar fashion as using a chopper and a locking amplifier to remove noise in some optical experiments. Cells apparently could mistake the pulsating NIR light sources for other nearby cells and extend processes towards them [168–170; 172].

The effect could be very similar when cortical neurons are subjected to distant pulsating light sources which can well be justified while using chopped CW light. However it would seem highly unlikely that cellular sensors could respond to the very high pulsating frequency of about 100MHz during femtosecond operation. It is very possible that there could be some sort of an undersampling by the cellular sensors and when using 100Mhz pulsating femtosecond source, the cells actually see a much lower frequency to which they could very well respond.

The percentage of attracted neurons in the CW case is slightly more than in the control case. Even though this increase was observed not to be statistically significant it is quite possible that even when a non pulsated CW light source is used neurons might display some weak attraction towards it. This postulate is however very difficult to ascertain.

If cells do communicate between themselves using light they would indeed need a source of light. This light should either be generated by the cell itself or obtained externally. Both these hypothesizes have been equally supported. It is well established that cells can produce weak optical signals called biophotons [173; 174]. It has also been established that these biophotons are used for intercellular communication [175; 176] by the cells. For example it has been shown that Inducer Caco-2 cells when exposed to H_2O_2 induced chemical and morphological changes in Detector Caco-2 cells placed in separate transparent containers near the inducer cells but were not exposed to H_2O_2 [177]. It was hypothesized that since the containers were mechanically and electrically separated the only way the cells could communicate was through light (biophotons) through the transparent containers. Cells also could receive and subsequently scatter the ambient light to use in intercellular communication. In a previous work it was proposed that the light scattering by perinuclear particles mediated long range attraction, which appeared to enable the aggregation of 3T3 cells [170]. These cells were able to detect and move toward the most visible cells from a distance of many cell diameters.

If cells do communicate between themselves using light they should also be able to sense and subsequently respond to the optical communication signal. The optical sensors could possibly be the deep brain photoreceptors (opsin-3). Contrary to previous belief

that biological optical receivers are confined to the retina and the pineal gland, a number of deep brain nonretinal/nonpineal opsins have been studied in last few years as natural photoreceptors and their expression in deep brain neurons are well established [167]. Light has been shown to trigger calcium-dependent exocytosis in primary chicken telencephalic neurons, building up plasma membrane [166]. Opsins present in the neurons were implicated as the optical detectors responsible for this effect. In addition the centrosomes in the cell body of cells were also suggested as possible infrared detectors [178]. It has also been suggested that a more general function of the centrosome would be to integrate exogenous optical signals and send response signals along microtubules to various sites within the cell [179]. In the case of neurons it is possible that the transparent axon, with a refractive index higher than that of the surrounding media, acts like an optical conduit or like an optical fibre to relay the optical signals received from the distant pulsed sources by the growth cone onto the centrosomes in the cell body which later induces growth responses.

Even though all the above arguments strongly point to crosstalk incurred in the intercellular communication as the possible reason behind the observed effects the involvement of other mechanisms cannot be fully ruled out.

When optical pulses are used, laser-induced pressure waves (PW) can be generated. At the right intensity levels, it has been shown that these can induce pore formation and thus able to promote exocytosis [180]. The mechanisms involved in generation of PW are optical breakdown, ablation and rapid heating of an absorbing medium [181]. In the case of the chopped CW pulses, the culture medium is exposed to a rapid temperature increase of $\sim 1.5^0$C that is quickly dissipated during the chopped condition, generating thus PW. When considering the FS pulses, it has to be considered first that water has an optical break down of 200 nJ/pulse and the ablation threshold is ~600pJ/pulse [182]. These are, orders of magnitude higher than the energy per pulse used in our FS experiments (40pJ/pulse). However, our FS pulses are capable of inducing an optical pressure of the order of 65KPa. This can mechanically induce noticeable surface tension changes in the culture medium or in the substrate [84]. If the PW are generated in the substrate, these can be manifested as vibration waves that follow the repetition rate of the laser or a lower harmonic frequency. Therefore, although due to different reasons, PW might also be considered as a mechanism responsible for inducing axonal growth towards the position of the pulsed light focused beam.

In FS regime, an alternative mechanism to PW could be the ionization of the media through multiphoton processes caused by highly focused FS pulses which may be inducing a localized electrical tension that could be sensed by the neuron.

There is a high degree of speculation in all the arguments presented above as to why cellular processes should extend towards distantly placed pulsating NIR light source. A consolidated effort is required to solve this puzzle.

Even though similar works have been performed before the present work could be deemed more significant since these have been demonstrated with neurons and moreover using primary cells rather than cell lines. The significance of this work can also be assessed by the fact that a systematic comparison of all the operating regimes (CW, pulsating CW and Femtosecond) had not been performed before.

These results, obtained using primary neuronal cell cultures, represent what we believe is an interesting discovery demonstrating the ability of axons trajectories to be controlled remotely by the use of pulsating light sources. The fact that the beam spot is located at

some distance from the axonal growth cone reduces any eventual photodamage. The use of primary cultures stresses the viability of the method raising interesting possibilities for eventual biomedical applications. There are many parameters (wavelength, focused spot size, intensity, pulse duration, culture medium, age of neurons, etc.) that can be varied and that could result in a more robust and enhanced methodology to achieve axonal guidance. The identification of the molecular mechanisms involved could unveil new possibilities in the field of neuronal guidance during normal development. In the long term, this optically-based method has the potential to open up new alternatives in the search of effective therapies for neural and brain repair.